

**Abstracts of the Papers Published by the  
Staff Members of the Institute from  
July, 1976 to June, 1977**

**Nuclear Chemistry**

**Effect of  $\gamma$  Radiation on Gate Trigger Current of Thyristors.** Y. Izawa and R. Katano. *Bull. Inst. Chem. Res., Kyoto Univ.*, **55**, 20 (1977).—Experimental study on the  $\gamma$ -radiation effect in gate trigger current,  $I_{GT}$ , of small current thyristors (2A class) has been performed. The gate trigger current is sensitively increased by  $\gamma$  radiation and the stability of the thyristor is improved. The increase in  $I_{GT}$  is proportional to the  $\gamma$ -radiation dose and is not deteriorated by heat treatment at 200°C for 1000 h.

**Superconducting Transition Temperature of Technetium and Lead.** M. Kurakado, T. Takabatake, and H. Mazaki. *Bull. Inst. Chem. Res., Kyoto Univ.*, **55**, 38 (1977).—Superconducting transition temperatures of technetium and lead were determined by means of resistive transition. Technetium samples were prepared by electrodeposition and reduction. Lead samples were prepared by the usual vacuum evaporation. The transition temperatures are  $7.46 \pm 0.05$  K for technetium and  $7.257 \pm 0.01$  K for lead.

**Monte Carlo Calculations of Transmission of Electrons through Thin Foils.** T. Mukoyama and Y. Watanabe. *Bull. Inst. Chem. Res., Kyoto Univ.*, **55**, 46 (1977).—A Monte Carlo method to calculate transmission of electrons through thin foils is described. Angular deflection due to multiple scattering, energy loss by ionization, and fluctuation in energy loss are taken into account. The calculations have been made for electrons normally incident on thin aluminum foils of various thicknesses. The results obtained are in fairly good agreement with other calculation and with the experimental results.

**A Pressurized Multiwire Proportional Counter for Electrons.** T. Kitahara, Y. Isozumi, and S. Ito. *Nuclear Instr. and Meth.*, **140**, 263 (1977).—A pressurized multiwire proportional counter assembly has been developed. The central counter is surrounded by twelve ring counters in a high-pressure tank, in which a gas mixture (90% Ar-10% CH<sub>4</sub>) is filled up to 30 kg/cm<sup>2</sup>. In order to improve the energy resolution for electrons, pulses from ring counters are used as the anticoincidence gating pulses for the pulses from the central counter and the risetime-selection circuit is built in the central-counter channel. The assembly is tested with conversion electrons from <sup>109</sup>Cd, <sup>113</sup>Sn, and <sup>137</sup>Cs sources mounted inside the central counter. The fwhm value of the 624 keV electrons from <sup>137</sup>Cs is achieved as 8.5%.

**Double K-Hole Creation in the 145 keV Internal Conversion of  $^{141}\text{Pr}$ .** S. Ito, Y. Isozumi, and S. Shimizu. *Phys. Lett.*, **59A**, 151 (1976).—By means of the X-ray-X-ray coincidence technique with two Si(Li) detectors, the probability of the double K-hole creation in the 145 keV M1 internal conversion of  $^{141}\text{Pr}$  was estimated. The energy displacement of the  $K_{\alpha}$  hypersatellite line was also measured.

**Stopping Powers of Be, Al, Ti, V, Fe, Co, Ni, Cu, Mo, Rh, Ag, Ta, and Au for 28.8 MeV Alpha Particles.** R. Ishiwari, N. Shiomi, and S. Shirai. *Bull. Inst. Chem. Res., Kyoto Univ.*, **55**, 60 (1977).—Stopping powers of Be, Al, Ti, V, Fe, Co, Ni, Cu, Mo, Rh, Ag, Ta, and Au for 28.8 MeV alpha particles have been measured with a silicon detector and associated electronic equipment. It has been confirmed that the stopping power for alpha particles divided by 4 is higher than that for protons of the same velocity. The deviations are from 2.4 to 4 percent.

**Stopping Powers of Al, Ni, Cu, Ag, and Ta for 8.78 MeV Alpha Particles.** R. Ishiwari, N. Shiomi, T. Kinoshita, and F. Yasue. *Bull. Inst. Chem. Res., Kyoto Univ.*, **55**, 68 (1977).—The stopping powers of Al, Ni, Cu, Ag, and Ta have been measured by using the absorber wheel technique and a silicon detector. In order to examine the possible nonuniformity of the sample foil, the alpha particle beam was made to scan in two directions, *i.e.* parallel and perpendicular to the rolling direction of the foil. The agreement between the measurements of two directions was proved to be satisfactory. The present results were divided by 4 and reduced to 2.0 MeV and compared with the proton data from the table of Bichsel. It turned out that the data for alpha particles are by 1.4–3.4 percent higher than those for protons.

**Kéage Laboratory of Nuclear Science, Decennial Report 1966–1976.** T. Yanabu. *Bull. Inst. Chem. Res., Kyoto Univ.*, **55**, 74 (1977).—The activities of the Kéage Laboratory of Nuclear Science in the period from 1966 to 1976 are summarized and reviewed. This report is a continuation of a report written by K. Kimura in 1965. Layout of the laboratory, development of nuclear instrumentations, researches in nuclear physics and chemistry, are grouped into sections and the trends in the history of the laboratory are described.

**Continuous Energy Spectra of Alpha-Particles from  $^{11}\text{B}(p, \alpha)^8\text{Be}$  Reaction.** K. Fukunaga, T. Ohsawa, S. Kakigi, S. Tanaka, and N. Fujiwara. *J. Phys. Soc. Japan*, **42**, 725 (1977).—Spectra of alpha-particles emitted from the  $^{11}\text{B}(p, \alpha)^8\text{Be}$  are obtained at the angle of  $90^\circ$  in the energy range from 6.5 to 7.3 MeV and also in the angular range from  $20^\circ$  to  $160^\circ$  at the proton energy of 7.26 MeV. The energy spectra are analyzed by a resonance formula. The width corresponding to the first excited state of  $^8\text{Be}$  varies with the incident proton energy and the observing angle. The observed width is narrow at the resonance of the intermediate system of  $^{12}\text{C}$ .

**Empirical Rules on the Attenuation of Quasifree Scattering in Nucleon-Deuteron Breakup in the Energy Range from 15 to 156 MeV.** N. Fujiwara. *J. Phys. Soc. Japan*, **42**, 1797 (1977).—Simple empirical rules are in existence on the

$(\sigma_{\text{exp}}/\sigma_{\text{sm}})$ , the ratio of the experimental cross section for p-p and p-n quasifree scattering (QFS) to the one calculated with the spectator model. (1) The ratio for p-n QFS,  $(\sigma_{\text{exp}}/\sigma_{\text{sm}})_{p1-n2}$ , depends only on the relative energy  $E_{n2-p3}$  between scattered neutron and spectator proton, namely  $(\sigma_{\text{exp}}/\sigma_{\text{sm}})_{p1-n2}=f(E_{n2-p3})$ . (2) The ratio for p-p QFS,  $(\sigma_{\text{exp}}/\sigma_{\text{sm}})_{p1-p2}$ , depends on the relative energies  $E_{p1-n3}$  and  $E_{p2-n3}$  and is expressed by a product form of the same function for p-n QFS, namely  $(\sigma_{\text{exp}}/\sigma_{\text{sm}})_{p1-p2}=f(E_{p1-n3})\times f(E_{p2-n3})$ . (3) Further, the function  $f(E)$  is expressed by the deuteron wave function in momentum space.

**Test of Proton-Induced  $^2\text{H}$  Breakup: Investigation for the Special Kinematic Condition of Collinearity.** N. Fujiwara, H. Hourany, H. Nakamura-Yokota, F. Reide, and T. Yuasa. *Phys. Rev., C*, **15**, 4 (1977).—The breakup of  $^2\text{H}$  induced by 156 MeV protons has been studied in the  $(p, 2p)$  and the  $(p, pn)$  reactions in the kinematically complete measurement with the unique kinematic condition: The three nucleons are collinear in the center of mass system of three nucleons in the final state. Also we performed experiments having neighboring kinematic conditions. The  $d^3\sigma/d\Omega_1 d\Omega_2 dE_1$  spectrum gives a peak in the region far from the final-state interaction and the true quasifree interaction regions. In this region of interest  $d^3\sigma/d\Omega_1 d\Omega_2 dE_1$  is calculated by a model derived from the fixed-scattering-center approximation proposed by L'Huillier and Ballot with Benoist-Gueutal. The model gives a smooth minimum, while the experimental peak is very sharp and sensitive to  $\theta_3$ . The fixed-scattering-center approximation explains the present experimental  $d^3\sigma/d\Omega_1 d\Omega_2 dE_1$  spectrum in the entire region fairly well except at this peak. Because of this, we consider this peak difficult to explain by the fixed-scattering-center approximation to the Faddeev equation solution. This peak is similar to that observed by Lambert *et al.* at 23 MeV.

**Etude des Caractéristiques d'un Grand Compteur à Scintillateur Plastique Destiné à la Localisation et à la Mesure du Temps de vol des Neutrons de 2 à 200 MeV.** E. Hourany, S. Kakigi, F. Reide, and T. Yuasa. *Annuaire de l'Institut de Physique Nucléaire (ORSAY)*, N.53 (1976).—The resolution for the time of flight and the localization have been studied with various particles in the energy regions from 1.0 MeV up to 140 MeV and neutron detection efficiency has been measured at 5, 10, and 14.6 MeV as a function of the threshold energy. A system of hodoscopes has been settled to improve the time resolution.

**Continuous Energy Spectra of Alpha-Particles from  $^{11}\text{B}(p, \alpha)^8\text{Be}$  Reaction.** K. Fukunaga, T. Ohsawa, S. Kakigi, S. Tanaka, and N. Fujiwara. *J. Phys. Soc. Japan*, **42**, 725 (1977).—Spectra of alpha-particles emitted from the  $^{11}\text{B}(p, \alpha)^8\text{Be}$  are obtained at the angle of  $90^\circ$  in the energy range from 6.5 to 7.3 MeV and also in the angular range from  $20^\circ$  to  $160^\circ$  at the proton energy of 7.26 MeV. The energy spectra are analyzed by a resonance formula. The width corresponding to the first excited state of  $^8\text{Be}$  varies with the incident proton energy and the observing angle. The observed width is narrow at the resonance of the intermediate system of  $^{12}\text{C}$ .

## Analytical Chemistry

**A Highly Sensitive Spectrophotometric Determination of Palladium with Chromal Blue G and Cetyltrimethylammonium Chloride.** K. Uesugi and T. Shigematsu. *Anal. Chim. Acta*, **84**, 377 (1976).—A new spectrophotometric method for the determination of palladium with chromal blue G (Color Index 43835) and cetyltrimethylammonium chloride is described. The sensitivity of the color reaction between palladium and chromal blue G is greatly increased in the presence of cetyltrimethylammonium chloride. The palladium complex has maximal absorbance at pH 3.2–3.8 and at 670 nm. Beer's law is obeyed over the range 0.08–1.4 p.p.m. palladium; the molar absorptivity is  $1.01 \cdot 10^5 \text{ l mol}^{-1} \text{ cm}^{-1}$  at 670 nm and the sensitivity is  $1 \cdot 10^{-3} \text{ } \mu\text{g Pd cm}^{-2}$ . The mole ratio of palladium and chromal blue G in the complex in the presence of cetyltrimethylammonium chloride is 1:3. Only scandium interferes when sodium fluoride is used as masking agent.

**Coprecipitation of Cadmium with Calcite.** O. Fujino, T. Kumagai, T. Shigematsu, and M. Matsui. *Bull. Inst. Chem. Res., Kyoto Univ.*, **54**, 312 (1976).—The distribution of cadmium between precipitates of calcite and saturated aqueous solution was measured at 25°C to understand the distribution of cadmium in the bivalves. Calcite was precipitated from calcium bicarbonate solution by the gradual release of carbon dioxide. The cadmium ions were coprecipitated in calcite, obeying the logarithmic distribution law. The apparent distribution coefficient was decreased as  $\alpha$ ,  $\alpha'$ -dipyridyl increased, but the true distribution coefficient was found to be an almost constant value, 560. This value is fairly close to the ratio of solubility product constants  $K_{\text{calcite}}/K_{\text{CdCO}_3}$ , 890. This suggests that the deviation of the present solid solution from ideality is not very large.

**Coprecipitation of Cadmium with Aragonite.** T. Kumagai, O. Fujino, M. Matsui, and T. Shigematsu. *Bull. Inst. Chem. Res., Kyoto Univ.*, **54**, 320 (1976).—The coprecipitation behavior of cadmium during the precipitation of aragonite from calcium bicarbonate solution was investigated at 25°C. The distribution coefficient of cadmium between aragonite and solution phase increased with increasing concentration of magnesium chloride. This increment in distribution coefficient was caused by the increase of the ionic strength in the solution phase. The true distribution coefficient of cadmium is nearly independent of the concentration of chloride and magnesium ions at a constant ionic strength, and is found to be 44 at 0.5 of ionic strength.

**Thermodynamics of Adduct-Formation of Bis(3-trifluoroacetyl-*d*-camphorato)copper (II) with Pyridines.** T. Shigematsu, M. Matsui, Y. Sasaki, and M. Sakurada. *Bull. Inst. Chem. Res., Kyoto Univ.*, **54**, 335 (1976).—Thermodynamic data was obtained for the reaction in benzene solution of bis(3-trifluoroacetyl-*d*-camphorato) copper(II) with pyridines. The enthalpy change of the adduct formation with pyridine is  $-6.8 \text{ Kcal/mol}$  which is similar to that of  $\text{Cu}(\text{tfa})_2$ . The enthalpy changes of the adduct formation with  $\beta$ - and  $\gamma$ -picolines are unusually large. The  $\Delta H$  value of  $\alpha$ -picoline is  $-8.3 \text{ Kcal/mol}$ .

**Adduct-Formation Constants of Bis(3-trifluoroacetyl-*d*-camphorato)copper (II) with Lewis Bases.** T. Shigematsu, M. Matsui, Y. Sasaki, and M. Sakurada. *Bull. Chem. Soc. Japan*, **49**, 2325 (1976).—The formation constants of the mono-adducts of bis(3-trifluoroacetyl-*d*-camphorato)copper (II) with the Lewis bases, such as pyridine,  $\alpha$ -picoline,  $\beta$ -picoline,  $\gamma$ -picoline, isopropylamine, and *d*- and *l*- $\alpha$ -methylbenzylamine, were determined spectrophotometrically.

**Fluorometry.** T. Shigematsu. *Bunseki (The Analyst)*, 348 (1976), in Japanese.—Review.

**Fluorometric Determination of Selenium (IV) and Selenium (VI) in Sea Water and River Water.** O. Yoshii, K. Hiraki, Y. Nishikawa, and T. Shigematsu. *Bunseki Kagaku (Japan Analyst)*, **26**, 91 (1977), in Japanese.—A simple and convenient chemical separation procedure for determination of Se(IV) and Se(VI) by spectrofluorometric analysis is proposed and applied to the study of the valence state of Se(IV) and Se(VI) in sea water and river water. Immediately after the collection of water samples, (2–3) l of sample water was filtered through a 3  $\mu$  and a 0.3  $\mu$  pore-size Membrane filter successively. Thirty milligrams of Fe(III) as FeCl<sub>3</sub> was added to the sample water with continuously stirred and pH of the solution was maintained to 5. After being allowed to stand for (2–3) hrs., the precipitate was filtered. By this time, Se(IV) was coprecipitated with Fe(OH)<sub>3</sub>, and Se(VI) was remained in filtrate completely. The precipitate was dissolved in (1–2) ml of concentrated hydrochloric acid and diluted to 25 ml with water. To remove Fe(III), an aliquot of the solution was taken, 3 ml of 1 M acetic acid was added to the solution, and pH of the solution was adjusted to 5 by adding saturated sodium acetate solution. The solution was extracted with 10 ml of 1 M capric acid-CHCl<sub>3</sub> solution. The aqueous layer was washed with CHCl<sub>3</sub>, and Se(IV) was measured by 2,3-diaminonaphthalene (DAN) fluorometric method [This Journal, **22**, 712 (1973)]. Selenium (VI) in the filtrate was concentrated by tellurium coprecipitation method. The filtrate was acidified to 1 M HCl, and (10–20) mg of Te(IV) solution, (100–300) g of hydrazine sulfate were added to this solution and boiled for 30 minutes at (80–100)°C. The ash-colored metallic tellurium was dissolved with nitric acid and (0.5–2) ml of perchloric acid, and evaporated to dryness. The residue was dissolved with 5 ml of 6 N HCl and boiled for 3 minutes and diluted to 25 ml with water. An aliquot of this solution was taken, and selenium was measured by DAN fluorometric method. In this procedure, the recovery of Se(IV) and Se(VI) were about up to 95%. Coastal seawater of Japan and river water has been found to contain (0.01–0.05)  $\mu$ g Se(IV)/l and (0.03–0.28)  $\mu$ g Se(VI)/l. The method of determination of particle size distribution of selenium in suspended matter was also proposed.

**Neutron-prompt  $\gamma$ -ray Spectrometry.** T. Shigematsu. *Kagaku (Chemistry)*, **32**, 495 (1977), in Japanese.—Review.

**A Highly Sensitive Spectrophotometric Determination of Gallium with Pontachrome Azure Blue B and Cetyltrimethyl-Ammonium Chloride.** K.

Uesugi and T. Shigematsu. *Talanta*, **24**, 391 (1977).—A new spectrophotometric method for the determination of gallium with Pontachrome Azure Blue B and cetyltrimethyl-ammonium chloride is described. The sensitivity of the color reaction between gallium and Pontachrome Azure Blue B is greatly increased in the presence of cetyltrimethyl-ammonium chloride. The gallium complex has maximal absorbance at 680 nm and pH 6.0–6.6. Beer's law is obeyed over the range 0.08–0.6 ppm of gallium; the molar absorptivity is  $1.39 \pm 10^5 \text{ l} \cdot \text{mole}^{-1} \cdot \text{cm}^{-1}$  and sensitivity  $4.9 \pm 10^{-4} \mu\text{g}/\text{cm}^2$ . The mole ratio of the complex, the formation constant and effect of interfering ions are described.

### Physical Chemistry

**Dielectric Dispersion of Cultured Lymphoma Cells (L5178Y) in Suspension: Determination of Membrane and Intracellular Electrical Properties by Means of a 'Double-Shell' Model.** A. Irimajiri, Y. Doida, T. Hanai, and A. Inouye. *Biophysical J.*, **17**, 167a (1977).—Frequency-dependent changes in the dielectric constant and conductivity of L5178Y cells suspended in culture media were measured over a range 0.01–100 MHz by a bridge method, and an attempt has been made to explain the observed dielectric behavior of cells by taking explicitly into consideration the involvement of large nuclei located in the cytoplasm. In fact, the gross dispersion curves were not simulated satisfactorily in terms of a 'single-shell' model such as employed thus far, whereas a 'double-shell' model in which one additional, concentric shell phase was incorporated into the 'single-shell' model gave a much better fit between the observed and the predicted dispersion curves. Based on the latter model, we analyzed the raw data of dielectric measurements to yield a set of plausible electric parameters for the lymphoma cell:  $C_M = 1.0 \mu\text{F}/\text{cm}^2$ ,  $C_N = 0.4 \mu\text{F}/\text{cm}^2$ ,  $\epsilon_k \approx 300$ ,  $\kappa_c/\kappa_a \approx 0.9$ , and  $\kappa_k/\kappa_c \approx 0.7$ . Here,  $C_M$  and  $C_N$  are the specific capacities of cytoplasmic and nuclear membranes;  $\epsilon$  and  $\kappa$  are dielectric constant and conductivity with subscripts  $a$ ,  $c$ , and  $k$  denoting respectively the extracellular, the cytoplasmic and the karyoplasmic phases.

**Dielectric Behavior of Yeast Cell Suspensions: Effects of Some Chemical Agents and Physical Treatments on the Plasma Membranes and the Cytoplasms.** K. Asami. *Bull. Inst. Chem. Res., Kyoto Univ.*, **55**, 283 (1977).—Dielectric measurements were made on suspensions of yeast cells treated with various chemical agents such as ionic and nonionic detergents, sodium tetraphenylborate, KI and gramicidins, and with various physical means such as heating, freezing-thawing and irradiation of VU light. Two different types of changes in the dielectric dispersion were observed by these treatments. For the treatments with nonionic detergents and sodium tetraphenylborate, the characteristic frequency of the dielectric dispersion was found to shift to lower frequencies without changing the limiting dielectric constant and conductivity at low frequencies, indicating a decrease in conductivity of the cytoplasm without remarkable changes in the conductivity and capacitance of cytoplasmic membranes. On the other hand, the dielectric dispersion was reduced by

the treatments with ionic detergents and physical means. Since the reduction was accompanied by a decrease in packed volume of the cells and by a leakage of the intracellular compounds, it is considered that the reduction is caused by remarkable increase in the conductivity of cytoplasmic membrane and decrease in the cell volume.

**Evaluation of a Conductometric Method to Determine the Volume Fraction of the Suspensions of Biomembrane-Bounded Particles.** A. Irimajiri, T. Hanai, and A. Inouye. *Experientia*. **31**, 1373 (1975).—A new method is proposed to determine the volume concentration of cells or isolated organelles in suspension by means of conductometry. The principle used for the conductometric method is that a ratio of the conductivity of the suspension to that of the continuous medium is expressed accurately as a certain function of the volume concentration of the suspended particles. As the practice of this conductometric method, the volume fractions of suspended particles for some suspensions composed of mouse lymphoma L5178Y, synaptosomes, and rat liver mitochondria were determined with sufficient reliability, and were in good agreements with the values estimated by the space-marker method with  $^{14}\text{C}$ -inulin. Supported by the fact of satisfactory agreements between the results of some independent techniques compared, the conductometric method is recommended as a simple, nondestructive, and reliable tool for determining the volume fraction of the suspensions of membrane-limited particles of biological relevance. It requires only conductivity measurements on a suspension and its continuous medium.

**Dielectric Properties of Yeast Cells: Effect of Some Ionic Detergents on the Plasma Membranes.** K. Asami, T. Hanai, and N. Koizumi. *J. Membrane Biol.*, **34**, 145 (1977).—Dielectric measurements were made on suspensions of yeast cells treated with two homologous series of sodium alkyl ( $\text{C}_8$ ,  $\text{C}_{10}$ ,  $\text{C}_{12}$ ,  $\text{C}_{14}$ ) sulfonates and alkyl ( $\text{C}_8$ ,  $\text{C}_{10}$ ,  $\text{C}_{12}$ ,  $\text{C}_{14}$ ,  $\text{C}_{16}$ ,  $\text{C}_{18}$ ) benzyl dimethyl ammonium chlorides over a frequency range of 10 kHz to 100 MHz. Dielectric dispersions observed for the suspensions of intact yeast cells are found to be reduced by treatment with these detergents, the reduction being accompanied by a decrease in packed volume of the cells and by a leakage of intracellular compounds. The reduction of dielectric dispersions is considered to be caused by a decrease in volume of the cells in suspensions and an increase in conductivity of the cell membranes. An effect of the alkyl chain length of the detergents on the reduction of dielectric dispersions is also examined for these ionic detergents. The reducing effect shows the maximum at the alkyl chain  $\text{C}_{14}$  for sodium alkyl sulfonates and at  $\text{C}_{16}$  for alkyl benzyl dimethyl ammonium chlorides. These results are consistent with hemolysis and bactericidal activity.

**Dielectric Approach to a Suspension of Membrane-Bounded Particles, and the Application to Biological Suspensions.** H. Hanai and K. Asami. *Maku (Membrane)*, **2**, 175 (1977), in Japanese.—Dielectric approach to disperse systems is of practical as well as of fundamental importance since information on the internal structure and properties of the disperse systems can be obtained either without disturbing the systems or while maintaining them in any desired state or condition during the measurement. In this review article, a dielectric theory and the application are

explained for a suspension that spheres covered with a shell phase are dispersed in a continuous medium. Such a kind of structure for a suspension including shell-spheres can readily be found in biological suspensions such as erythrocytes, bacteria and cultured cells dispersed in appropriate aqueous media. The systematic analysis of the dielectric data for the systems leads to reasonable estimation of dielectric constants and electrical conductivities of the membranes and the inner phase of these dispersed globules in their intact states.

The contents of this treatise are as follows: 1. Introduction. 2. Dielectric theory of a suspension of spherical globules covered with a shell phase. 3. Pattern of the dielectric relaxation, and the expressions of the observable dielectric parameters. 4. Approximate expressions for the case of a very thin and less conducting shell phase. 5. Some characteristics of the dielectric relaxation. 6. Elementary explanation for very high dielectric constants due to the less conducting shell phase. 7. Simplified approximate expressions and their application to observed data on dielectric relaxations. 8. Application technique of the general expression to the observed data (curve-fitting procedure). 9. Conclusion.

**Effect of Illumination on the Squid Rhodopsin Membrane at Oil-Water Interface.** M. Takagi, K. Asami, T. Hanai, and U. Kishimoto. *Science Reports, College of General Education, Osaka Univ.*, **24**, 69 (1975).—Illumination of the squid rhodopsin membrane formed at an oil-water interface caused a remarkable change in the phase boundary potential. The potential change caused by the flash illumination showed a fast decrease and a slow recovery. The potential displacement appeared without any significant latency and reached the maximum at 3 sec after the flash illumination. The maximum change was decreased as the flash illumination was repeated. However, the potential behavior was unchanged irrespective of the repeated illumination. It was confirmed that the change in the electric potential attributed not to those in pH, redox potential and ionic activities in the bulk aqueous phase, but to those in rhodopsin molecules at the oil-water interface. The maximum change was observed at the neutral pH region of the aqueous phase. This is in accord with the pH dependent regeneration of cattle rhodopsin.

**Experiments on Black Lipid Membranes, and the Application.** T. Hanai. *Tanpakushitsu, Kakusan, Koso, Ge (Protein, Nucleic Acid and Enzyme. Supplement Experiments on Biological Membranes)*, 199 (1974), in Japanese.—Experimental techniques are described in detail on the formation and the physico-chemical measurements of underwater black lipid films (bilayer lipid membranes). 1. Materials and Apparatus. Careful preparation is introduced for electrodes, brushes, materials, and specialized techniques for the cell and the apparatus used. 2. Preparation of the Film Forming Solution. 3. Formation of the Thin Black Lipid Films. Some very important knock such as pre-painting, underwater smoothing, and one-stroke setting of the spreading solution is explained in detail. 4. Electrical Measurements of D. C. and A. C. Characteristics. Some comparisons and comments are given among various electrical measurements. 5. Membrane Potential Measurements.



**Effects of the Dynamical Scattering on the Molecular Images in High Resolution Electron Microscopy.** K. Ishizuka and N. Uyeda. *Bull. Inst. Chem. Res., Kyoto Univ.*, **55**, 260 (1977).—The wave functions and the scattering amplitudes of the crystal of chlorinated Cu-phthalocyanine were calculated based on the multi-slice formula of the dynamical scattering theory. A direct correlation between the intensity of the wave function and the specimen structure was obtained for the crystal of the thickness below 180 or 120 Å for 500 or 100 kV electron respectively. Molecular images based on the dynamical scattering were synthesized by taking spherical aberration and defocusing effects into account. Although the condition for the kinematical approximation was not satisfied, the images similar to the kinematical ones were obtained at the Scherzer focus for the crystal of the thickness below 100 Å for both 500 kV electrons ( $C_s \times 1.0$  mm) and 100 kV electrons ( $C_s \times 1.4$  mm).

**Visualization of Molecular Structures; World through High Resolution Electron Microscopy.** N. Uyeda. *Bunseki (The Analyst)*, 236 (1977), in Japanese.—Review.

**LEED-AES Study of the Oriented Adsorption of Tetracyanoethylene on Potassium Chloride.** H. Saijo, N. Uyeda, and E. Suito. *J. Chem. Soc., Faraday Trans. II*, **73**, 517 (1977).—The adsorption state of tetracyanoethylene (TCNE) on the (001) cleavage face of KCl was studied by means of LEED combined with AES. The LEED pattern did not show any change in the arrangement of diffraction spots after the adsorption of TCNE molecules, although variations in their intensities were observed, but the intensity of the AES peak from potassium decreases remarkably on adsorption. It was deduced that four CN groups of each TCNE molecule are located directly over potassium ions specifically while less than one quarter of the chlorine ions are covered by C=C groups of TCNE with random orientation. The adsorption state of TCNE on KCl is discussed in relation to the epitaxial nucleation of a crystalline film of a similar compound, such as 7, 7', 8, 8'-tetracyanoquinodimethane (TCNQ). The surface stoichiometry of KCl crystal before the adsorption was confirmed by AES.

**Structure Analysis of a New Type of Vanadium Oxide by High Resolution Electron Microscopy.** Y. Fujiyoshi, K. Ishizuka, and N. Uyeda. *J. Electron Microsc.*, **26**, 47 (1977).—High resolution electron microscopy was applied to structure determination of new polytypes of vanadium oxide. The positions of apical oxygens were determined directly in the lattice images of one polytype.

**Visualization of Oxygen Atoms by Electron Microscopy.** N. Uyeda, T. Kobayashi, K. Ishizuka, and Y. Fujiyoshi. *Kagaku (Chemistry)*, **32**, 290 (1977), in Japanese.—Review.

**High Resolution Image Contrast and Chemical Structure.** N. Uyeda, T. Kobayashi, K. Ishizuka, Y. Fujiyoshi, and K. Kobayashi. *Proc. Sixth European Congr. Electron Microsc.*, Jerusalem, **1**, 79 (1976).—The possibility of electron microscopy to determine the chemical configuration is considered on the basis of some past ex-

periences and recent achievement for organic and inorganic crystals. It has become clear that the observation of high resolution images can make a certain contribution to the structure determination,—the atomic parameters can be directly assigned from them.

**Powder Characteristics and Its Measurement.** M. Arakawa. *Seramikkusu (Ceramics)*, 12, 399 (1977), in Japanese.—Powder characteristics and its measurement methods are reviewed in Japanese.

**The Vibrational Spectra of Tetracyanothiophene.** J. Nakanishi and T. Takenaka. *Bull. Chem. Soc. Japan*, 50, 36 (1977).—The polarized infrared and far-infrared spectra of the tetracyanothiophene crystals were recorded by means of the normal and oblique incidence of radiation upon the (001) and (20 $\bar{1}$ ) sample planes. The Raman spectra of the powdered sample and of a saturated solution in acetonitrile or 1,2-dichloroethane were also obtained. The observed bands were experimentally classified into the symmetry species of the free molecule (the point group  $C_{2v}$ ) under the assumption of an oriented gas model. Assignments of the observed bands to individual fundamental vibrations were carried out with the aid of the spectral data of the analogous molecules and the normal coordinate analysis of the in-plane vibrations, which was made with a modified Urey-Bradley force field.

**Origin of Foreign and Japanese Ambers Studied by Elemental Analyses and Infrared Spectroscopy.** T. Fujinaga, T. Takenaka, and T. Muroga. *Bunseki Kagaku (Japan Analyst)*, 25, 795 (1976), in Japanese.—The aim of the present work was to investigate the course of cultural exchange from the interpretation of the results obtained by physical and chemical analyses of archaeological amber products excavated in Japan; elemental analyses and infrared spectroscopy were carried out and the results were discussed in the present paper. Geological specimens, the origins of which are well known, were collected from Kuji, Ashikajima, Choshi, Hatoyama, Nagasaki, Inubosaki, Toriakeura, Gifu, Fushun, Palmnicken, Dominica, and Dalmatia. Archaeological amber samples of unknown origin were excavated from Tomio-maryama old tomb, Ueno old tomb and Jionji-wakimoto old tombs in Nara and Awashimadai remains in Chiba. The composition of geological samples were found to be C : H : O = 43–208 : 70–350 : 4, and archaeological samples to be 19–56 : 29–91 : 4 from the results of elementary analyses. The infrared spectrum of individual amber showed a characteristic pattern depending upon its provenance as was reported in the previous report. The archeological amber samples from Tomio-maryama old tomb (bead), Ueno old tomb (bead) and Jionji-wakimoto old tombs (bead) T0079, T0216 were found to have the provenance of Kuji in Iwate. And the amber artifacts excavated from Awashimadai remains No. 3–1 and ST5511 were identified as Choshi origin.

From these results, it was concluded that the amber produced from Kuji were widely distributed in the Kinki-district at the Tumlus period.

**The Force of Interaction in a Monomolecular Film at Low Surface Pressure.** M. Matsumoto, C. Montandon, and S. Hartland. *Colloid and Polymer Sci.*, **255**, 261 (1977).—The London-van der Waals attractive constant between methylene groups is experimentally determined from measurements of the constant and small surface pressure of a monomolecular film, assuming the formation of two dimensional micelles. Electrostatic repulsion is eliminated by subtracting the surface pressures for two surface active materials having the same polar groups but hydrocarbon chains of different lengths. Experimental values of the London-van der Waals attractive constant assuming a solid film are about  $5 \times 10^{-59}$  erg cm<sup>6</sup> which agrees well with the theoretical value.

**Molecular Configurations and Vibrational Spectra of Normal Fatty Acids.** S. Hayashi. *Gokuteion Kenkyushitsu Geppo, Kyoto Univ.*, No. 35, 1 (1977), in Japanese.—Review.

**Vibrational Spectra, Normal Coordinate Analyses, and Molecular Configurations of Crystalline Propionic Acid.** J. Umemura. *J. Mol. Struct.*, **36**, 35 (1977).—Temperature dependence of the IR spectra of crystalline propionic acid were examined in the temperature range 242–50 K. The intensities of most absorption bands increased on lowering the temperature, but some bands diminished until they disappeared at temperatures lower than about 120 K. Normal coordinate analyses indicate that the former bands are due to the stable *cis* dimer and the latter due to the less stable *trans* dimer which would be produced from the *cis* dimer by simultaneous proton transfer along two hydrogen bonds.

**Resonance Raman Spectra of Monolayers of a Surface-Active Dye Adsorbed at the Oil-Water Interface.** T. Nakanaga and T. Takenaka. *J. Phys. Chem.*, **81**, 645 (1977).—Resonance Raman spectra have been recorded for a monolayer of a surface-active dye, Suminol Milling Brilliant Red BS (abbreviated as BRBS), adsorbed at the interface between carbon tetrachloride and an aqueous solution by using a previously proposed method of total reflection of the exciting light at the interface. Theoretical considerations of the Raman scattering activity due to an evanescent wave in the total reflection have been made with a model of uniaxial orientation suitable for the BRBS molecule at the interface. From polarization measurements of the resonance Raman spectra at various concentrations of BRBS in the aqueous solution, the changes in intensity ratios of polarized Raman bands were found to have some correspondence to the change in the interfacial pressure. It was therefore concluded that the BRBS molecules were almost freely oriented in the monolayer at lower interfacial pressure, while the planes of the molecules showed a tendency to subtend an angle with the interface at higher interfacial pressure.

**Resonance Raman Spectroscopic Studies of Monomolecular Layers Adsorbed at the Oil-Water Interface.** T. Takenaka. *Kagaku no Ryoiki, Zokan (J. Japan. Chem.)*, **115**, 61 (1977), in Japanese.—The nature of the orientation of surfactants in monolayers adsorbed at the liquid-liquid or liquid-gas interfaces is one

of the most fundamental problems of surface chemistry. This is a review article describing a resonance Raman spectroscopic studies of monomolecular layers adsorbed at the interface between carbon tetrachloride and aqueous solution. The contents of the article are as follows;

1. Background of the problems.
2. Application of resonance Raman effect.
3. Total reflection methods of Raman spectral measurements of monomolecular layers adsorbed at the liquid-liquid interface.
4. Results and discussions.
  - 4.1 Complexes of surfactants with dyestuffs.
  - 4.2 Surface-active dyestuffs.
5. Postscript.  
References.

**Molecular Orientation in Surface Thin Films—Studies by Infrared and Raman Spectra.** T. Takenaka. *Maku (Membrane)*, 2, 25 (1977), in Japanese.—This is a review article describing infrared and Raman spectroscopic studies of the molecular orientation in thin films at various interfaces. The contents of the article are as follows;

1. Introduction.
2. ATR and specular reflection methods.
3. Molecular orientations in built-up films.
  - 3.1 Built-up films of fatty acids and their metal salts.
  - 3.2 Built-up films of stearamide.
4. Molecular orientations in thin films adsorbed at the solid-liquid interface.
5. Molecular orientations in monolayers adsorbed at the liquid-liquid interface.
6. Postscript.  
References.

**Simultaneous Proton Transfer in Hydrogen-Bonded Dimeric Systems in Crystalline State.** S. Hayashi and J. Umemura. *26th International Congress of Pure and Applied Chemistry, Tokyo*, 2, 587 (1977).—Infrared and Raman spectra of various carboxylic acids, which form hydrogen-bonded dimer in crystalline state, were obtained in the temperature range from room to liquid-helium temperatures. Great temperature dependences were observed in their spectra, especially in the frequency regions of the characteristic absorptions due to the hydrogen-bonded groups and some vibrations coupled strongly with the modes of the groups. The temperature dependences have been interpreted as due to the coexistence of two molecular configurations which would be led to each other by simultaneous transfer of both protons of dimers along the hydrogen bonds.

**Infrared Spectroscopic Analysis on the Rosins of Genus Pinus.** S. Oohata, T. Shidei, T. Muroga, and T. Takenaka. *Nippon Ringakkaishi (J. Japan Forestry Soc.)*, 59, 122 (1977), in Japanese.—To find an effective method for classification of the Genus *Pinus*, rosins of 14 pine species were examined by means of infrared spectro-

copy. Though the absorption spectra of all the rosins were similar as a whole, a careful examination indicated that there were some differences among them. From the comparison of the differences in seven wavenumber regions, the pines were classified into six groups, indicating a good correlation with the classification by Shaw. According to the present analysis, two species of *P. bungeana* and *P. longifolia* were classified in exceptional groups as previously mentioned by Ishii.

#### **Unimolecular Decomposition of Chemically Activated Methylallylether.**

T. Ibuki and Y. Takezaki. *International Journal of Chemical Kinetics*, **9**, 201 (1977).—The unimolecular decomposition of chemically activated methylallylether (MAE) formed by the cross combination of methoxymethyl and vinyl radicals was studied in the gas phase. The experimentally determined rate constant was found to be  $1.11 \times 10^8 \text{ sec}^{-1}$  at  $9.6^\circ\text{C}$  for the decomposition of MAE into propylene and formaldehyde. The decomposition of MAE via the six-center retro- "ene" type transition state is analyzed by using the RRKM unimolecular reaction theory. For the molecular parameter assignments of energized MAE, a model which contains one internal rotational mode is supported, and MAE decomposition is characterized by a tight complex model. The best agreement between experimental and theoretical results was found when a critical energy of  $40.1 \text{ kcal mol}^{-1}$  was used.

#### **Kinetic Study on the Synthesis of Alkali Formate from Carbon Dioxide and Hydrogen Catalyzed by Palladium (II) Chloride in an Aqueous Alkali Solution.**

K. Kudo, N. Sugita, and Y. Takezaki. *Nippon Kagaku Kaishi (J. Chem. Soc. Japan, Chem. and Ind. Chem.)*, 301 (1977), in Japanese.—It was found that palladium (II) chloride is a highly active catalyst for the synthesis of alkali formate from carbon dioxide and hydrogen in an aqueous alkali solution under pressure. For example, potassium formate, in 82.6 mol% yield, was obtained under the following condition: pressure of carbon dioxide being 40 atm, pressure of hydrogen being 106 atm, concentration of palladium (II) chloride being 1.0 g/l, concentration of potassium hydroxide in aqueous solution being 1.9 mol/l, temperature being  $240^\circ\text{C}$ , and period of reaction being 3 hrs.

The rate equation derived on the assumption of the reaction substances involving hydrogen-carbonate ion and active catalyst-hydrogen complexes, reasonably agreed with experimental results.

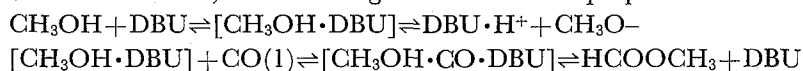
#### **Kinetic Study of Methyl Formate Synthesis from Methanol and Carbon Monoxide Catalyzed by 1,8-Diazabicyclo[5.4.0]undec-7-ene.**

K. Kudo, N. Sugita, and Y. Takezaki. *Nippon Kagaku Kaishi (J. Chem. Soc. Japan, Chem. and Ind. Chem.)*, 457 (1977), in Japanese.—It was found that 1,8-diazabicyclo[5.4.0]undec-7-ene (DBU) is an excellent catalyst for the synthesis of methyl formate from methanol and carbon monoxide under mild conditions.

The kinetic study of the carbonylation under pressure in methyl cellosolve solution showed that the rate of methyl formate formation is of the first order with respect to carbon monoxide pressure and to the concentration of methanol and DBU, and that the methyl formate decomposes to carbon monoxide and methanol with DBU under

the reaction, leading to the equilibrium.

Based on these results, the following mechanism was proposed:



The rate equation derived on this basis was in good agreement with the observed result.

## Inorganic Chemistry

**Fabrication of Transparent PbTiO<sub>3</sub> Glass-Ceramics.** T. Kokubo and M. Tashiro. *Bull. Inst. Chem. Res., Kyoto Univ.*, **54**, 301 (1976).—Transparent high permittive glass-ceramics are of interest for electro-optic and electro-luminescent applications. A method for fabricating glass-ceramics of this type by crystallization of glasses in the PbO·TiO<sub>2</sub>-AlO<sub>1.5</sub>SiO<sub>2</sub> system was investigated. Transparent glass-ceramics consisting primarily of a large amount of ferroelectric PbTiO<sub>3</sub> crystals with a perovskite-type structure were obtained from the composition region with PbO·TiO<sub>2</sub>/(AlO<sub>1.5</sub>SiO<sub>2</sub>)=2 and 1 ≤ AlO<sub>1.5</sub>/SiO<sub>2</sub> ≤ 2.3 in mole ratio. When a glass of the composition in the restricted region described above was heated from room temperature at a rate of 48°–300°C/hr, a metastable liquid-liquid phase separation first occurred, and as the results, the homogeneous structure of the glass changed into a microheterogeneous structure composed of glassy droplets of 16–18 nm in diameter. At higher temperatures, the phase-separated glass transformed into transparent glass-ceramics consisting primarily of PbTiO<sub>3</sub> crystals each having a diameter almost the same as that of the glassy droplets precursarily formed. It was assumed that precipitation of very-fine-grained PbTiO<sub>3</sub> crystal of a perovskite-type in the glass was assisted by the metastable phase separation in very fine scales, which had occurred precursarily.

**Crystallization Process of a LiTaO<sub>3</sub>-Al<sub>2</sub>O<sub>3</sub>-SiO<sub>2</sub> Glass.** S. Ito, T. Kokubo, and M. Tashiro. *Bull. Inst. Chem. Res., Kyoto Univ.*, **54**, 307 (1976).—A transparent glass-ceramic containing ferroelectric LiTaO<sub>3</sub> crystals is obtained from a glass of the composition 65 mol% LiTaO<sub>3</sub>, 17.5 AlO<sub>1.5</sub>, 17.5 SiO<sub>2</sub>, by heating from room temperature to 900°C at a rate of 5°C/min. To study effects of a metastable liquid-liquid phase separation on the subsequent crystal nucleation, structural changes of the glass during heat-treatment were investigated. The phase separation occurred from about 800° to 840°C. In its early stage (near 800°C), the phase-separated structure exhibited a microheterogeneity on 10 nm scale, whereas, in its advanced stage, it changed into a coarser structure composed of glassy droplets 0.5–1 μm in diameter, large enough to scatter the visible rays. The specimen with such a coarse structure showed opalescence. At 850°C, the opalescence disappeared. From 850°C, the glass started to crystallize, but remained transparent, at least, up to 900°C because the size of the individual crystal particles precipitated was less than 10 nm, small enough to minimize light scattering. The slow heating from 780° to 810°C which corresponded to the early stage of phase separation was found necessary to make the resulting glass-ceramic

transparent. It was concluded that the phase separation in its early stage enhanced the crystal nucleation.

**What is Transparency?** M. Tashiro. *Erekutoroniku Seramikusu (Electronic Ceramics)*, 8, Spring-2 (1977), in Japanese.—A review on transparency of glasses and ceramics.

**Infrared Transmission of  $(R_2O$  or  $R'O$ )-(TiO<sub>2</sub>, Nb<sub>2</sub>O<sub>5</sub> or Ta<sub>2</sub>O<sub>5</sub>)-Al<sub>2</sub>O<sub>3</sub> Glasses.** T. Kokubo, M. Nishimura, and M. Tashiro. *J. Non-Crystalline Solids*, 22, 125 (1976).—The new families of aluminate glasses obtained by the present authors from their melts in the systems K<sub>2</sub>O-Ta<sub>2</sub>O<sub>5</sub>-Al<sub>2</sub>O<sub>3</sub>, Na<sub>2</sub>O-K<sub>2</sub>O-Ta<sub>2</sub>O<sub>5</sub>-Al<sub>2</sub>O<sub>3</sub>, K<sub>2</sub>O-Cs<sub>2</sub>O-Ta<sub>2</sub>O<sub>5</sub>-Al<sub>2</sub>O<sub>3</sub>, K<sub>2</sub>O-Nb<sub>2</sub>O<sub>5</sub>-Al<sub>2</sub>O<sub>3</sub>, Na<sub>2</sub>O-K<sub>2</sub>O-TiO<sub>2</sub>-Al<sub>2</sub>O<sub>3</sub>, BaO-TiO<sub>2</sub>-Al<sub>2</sub>O<sub>3</sub>, BaO-ZrO<sub>2</sub>-TiO<sub>2</sub>-Al<sub>2</sub>O<sub>3</sub> and Na<sub>2</sub>O-K<sub>2</sub>O-BaO-ZrO<sub>2</sub>-Ta<sub>2</sub>O<sub>5</sub>-TiO<sub>2</sub>-Al<sub>2</sub>O<sub>3</sub> showed high transmissions of visible and infrared (IR) radiation ranging from 0.4 to about 6 μm, as well as high refractive indices up to 2.0. Their physical and chemical properties such as glass-forming ability, softening temperature, hardness and hygroscopicity were comparable to conventional silicate glasses. These properties are useful for IR applications. The cause of the high IR transmission of the aluminate glasses was interpreted in terms of the masses of the constituent cations and the single bond strengths of the cations with oxygen ions.

**Magnetic Relaxation in Fe<sub>3</sub>O<sub>4</sub> and Ferrites.** K. Iwauchi, N. Koizumi, K. Kiyama, and Y. Bando. *Bull. Inst. Chem. Res., Kyoto Univ.*, 54, 255 (1976).—Magnetic permeability and loss tangent ( $\tan \delta$ ) of Fe<sub>3</sub>O<sub>4</sub> and some ferrites were measured in the frequency range of 100 KHz to 1 MHz and the temperature range of 4.2 to 300 K with a transformer bridge by using the three terminal method. While  $\gamma$ -Fe<sub>2</sub>O<sub>3</sub> which has no Fe<sup>2+</sup> ion showed no peak in  $\tan \delta$ - $T$  curve, Fe<sub>3</sub>O<sub>4</sub> showed a peak in  $\tan \delta$  near 40 K. MnZn ferrite with Fe<sup>2+</sup> ions showed two peaks in  $\tan \delta$  near 30 and 150 K. The peak near 30 K was considered to be caused by the hopping of electron between Fe<sup>2+</sup> and Fe<sup>3+</sup> ions and the peak near 150 K by the electronic process of Mn ions.

**Crystal Growth of Molybdenum Oxides by Chemical Transport.** Y. Bando, Y. Kato, and T. Takada. *Bull. Inst. Chem. Res., Kyoto Univ.*, 54, 330 (1976).—Single crystals of MoO<sub>2</sub>, MoO<sub>3</sub> and Mo<sub>n</sub>O<sub>3n-1</sub> (n=4, 8, 9) were grown by chemical transport using TeCl<sub>4</sub> as transport agent. The electrical resistivities of the grown crystals were measured from liquid nitrogen temperature to room temperature.

**Mass Spectrometric Study on Chemical Transport Reaction.** M. Kyoto, Y. Bando, and T. Takada. *Chemistry Lett.*, 595 (1977).—In order to study closed-tube chemical transport reaction process, a mass spectrometer was coupled to a reaction tube. The gases in the ZnO-NH<sub>4</sub>Cl transport reaction were analyzed with this apparatus. The gas species were Zn, ZnCl<sub>2</sub>, N<sub>2</sub>, HCl, and NH<sub>3</sub>.

**Removal of Heavy Metal Ions from Waste Water by Magnetic Binding Materials.** T. Takada. *Kagaku (Chemistry)*, 31, 69 (1976), in Japanese.—Review.

**Study on Surface Structure of Inorganic Solid by Secondary Ion Mass Spectrometer.** M. Kyoto and Y. Bando. *Kagaku (Chemistry)*, **32**, 148 (1977), in Japanese.—Review.

**Study of Surface State by Mössbauer Spectroscopy.** T. Shinjo. *Kagaku (Chemistry)*, **supplement No. 70**, 183 (1977), in Japanese.—Applications of Mössbauer spectroscopy to surface problems are briefly surveyed. Surface effect on the local magnetic moment of ferromagnetic metals is mainly discussed and some experimental results are introduced concerning this problem.

**Formation and Properties of Iron Oxides and Hydroxides.** T. Takada. *Kagaku-Kogyo (Chemical Industry)*, 1145 (1976), in Japanese.—Review.

**Metallic-Antiferromagnetism of Non-Stoichiometric  $V_2O_{3+x}$  Studied by ( $^{57}\text{Fe}$ ) Mössbauer Effect.** Y. Ueda, K. Kosuge, S. Kachi, T. Shinjo, and T. Takada. *Mat. Res. Bull.*, **12**, 87 (1977).—It was confirmed by ( $^{57}\text{Fe}$ ) Mössbauer measurements that non-stoichiometric compositions  $V_2O_{3+x}$  ( $0.035 \leq X \leq 0.08$ ), which have metallic properties to lowest temperature, show a paramagnetic to anti-ferromagnetic phase transition at about 10 K.

**Invar Characteristics in  $(\text{Mn}_{1-x}\text{Cr}_x)\text{B}$  and  $(\text{Mn}_{1-x}\text{Fe}_x)\text{B}$ .** T. Shigematsu, T. Kanaizuka, and S. Kachi. *Nippon Kinzoku Gakkai-Shi (J. Japan Inst. Metals)*, **40**, 1131 (1976), in Japanese.—Thermal expansivity measurements were made on polycrystalline sintered  $(\text{Mn}_{1-x}\text{Cr}_x)\text{B}$  and  $(\text{Mn}_{1-x}\text{Fe}_x)\text{B}$ . These compounds show an anomalous thermal expansivity, similar to that of the invar alloys. Near the Curie temperature MnB shows a steep descent in the thermal expansivity curve, leading to a large negative thermal expansion coefficient. With the addition of Cr, the thermal expansion coefficient below the Curie temperature becomes smaller. The mean thermal expansion coefficient of  $(\text{Mn}_{0.88}\text{Cr}_{0.12})\text{B}$  from 100 K to 500 K is about  $1 \times 10^{-6}$  deg $^{-1}$ . This anomaly is explained as being a result of a large spontaneous volume magnetostriction. Magnetovolume effect of these materials are discussed on the basis of the band model of ferromagnetism.

**Surface Study of Fe by Mössbauer Effect.** J. Lauer, W. Keune, and T. Shinjo. *Physica*, **86-88B**, 1409 (1977).— $^{57}\text{Fe}$  Mössbauer experiments were performed to study the magnetic properties of an iron surface which was selectively enriched by vacuum deposition of a thin (5 Å)  $^{57}\text{Fe}$  layer and subsequently protected by a thick Cu film. The spectra at 4.2 K show that all Fe atoms near the surface are ferromagnetic, but the reduced hyperfine field suggests a partial decrease of the local magnetic moment.

**Removal of Heavy Metal Ions from Waste Water by Ferrite Formation.** T. Takada. *Sekiyu Gakkai-shi (Journal of the Japan Petroleum Institute)*, **19**, 9 (1976), in Japanese.—Review.



## Organic Chemistry

### Asymmetric Reduction of Iminium Salt with Chiral Dihydropyridines.

N. Baba, K. Nishiyama, J. Oda, and Y. Inouye. *Agr. Biol. Chem.*, **40**, 1441 (1976).—Asymmetric reduction of 1-phenylethylidenepyrrrolidinium perchlorate by the use of chiral Hantzsch ester and 1,4-dihydronicotineamide derivatives carrying (–)-(3*R*)-methyl group as chiral center was effected in non-polar and polar solvent media to give the corresponding *N*-(1-phenylethyl)-pyrrolidine of the *R*-configuration. The reduction was regiospecific with regard to the C+N double bond, and asymmetric yields were over the range of 2–10%.

### Studies on Insecticidal Constituents of *Juniperus recurva* Buch. J. Oda,

N. Ando, Y. Nakajima, and Y. Inouye. *Agr. Biol. Chem.*, **41**, 201 (1977).—The active insecticidal principles in the heartwood of *Juniperus recurva* were found to be thujopsene and 8-cedren-13-ol. Additional 12 sesquiterpenes were also detected in the neutral fraction of ether extracts.

### Self-Immolative Asymmetric Synthesis. III. Allylic Rearrangement of Optically Active Trichloroacetimidate. Y. Yamamoto, H. Shimoda, J. Oda,

and Y. Inouye. *Bull. Chem. Soc. Japan*, **49**, 3247 (1976).—The [3,3]sigmatropic rearrangement of (2*E*)-(1*R*)-1-methyl-3-phenyl-2-propenyl trichloroacetimidate to give *N*-[(2*E*)-(1*R*)-1-phenyl-2-butenyl]trichloroacetamide was effected thermally with nearly complete transfer of chirality *via* a doubly suprafacial transition state. The application of the self-immolative asymmetric synthesis to optically active carveols afforded carveylamines of the predicted configuration.

### Asymmetric Reduction of $\alpha, \beta$ -unsaturated Iminium Salt with *N*-glucopyranosyl-1,4-dihydronicotinamides. T. Makino, N. Baba, J. Oda, and Y. Inouye.

*Chemistry and Industry*, 277 (1977).—Reduction of  $\alpha, \beta$ -C=C double bond in the substrate iminium salt, 3,3,5-trimethyl-2-cyclohexylidene-pyrrolidinium perchlorate, was effected by the use of 1,4-dihydronicotinamides with glucopyranosyl residues on the 1-nitrogen atom, to give the optically active reduction end product, 3,3,5-trimethylcyclopentanone in 3–28% e.e. Both chemical and asymmetric yields of the ketone were found to be significantly higher with glucopyranosyldihydronicotinamide in which free hydroxyl groups are available in the reductant molecule than in those whose hydroxyl groups were masked. Thus, in runs where  $\beta$ -D-glucopyranosyl derivatives were used as reductant, both chemical yield and e.e. were doubled by deacetylation, with the dextrorotation of the product being unaltered. Whereas with the  $\alpha$ -anomeric counterparts employed, the deacetylation effected a slight improvement in chemical yield, but resulted in a dramatic reversal of the sign of rotation of the product with comparable asymmetric bias.

### Asymmetric Syntheses and Enzymic Reactions. J. Oda and Y. Inouye.

*Kakagu to Seibutsu*, **14**, 495 (1976), in Japanese.—Basic principles and general aspects of asymmetric synthesis were reviewed with special emphasis on the stereospecificity

in both asymmetric inductions and enzymic reactions.

**ent-9(8→15 $\alpha$ H)abeo-17-norkaur-8(14)-en-16-one.** T. Taga, T. Higashi, H. Iizuka, K. Osaki, M. Ochiai, and E. Fujita. *Acta Cryst.*, **B33**, 298 (1977).—The X-ray analysis of *ent-9(8→15 $\alpha$ H)abeo-17-norkaur-8(14)-en-16-one* is reported.  $C_{19}H_{28}O$ , orthorhombic,  $P 2_12_12_1$ ,  $a=23.69$  (4),  $b=8.058$  (12),  $c=8.132$  (12) $\text{\AA}$ ,  $Z=4$ . The two six-membered rings are in the chair form, and the five-membered ring is in an envelope conformation. All the rings in the molecule are somewhat distorted. Repulsion between the 1,3 diaxial methyl groups attached to ring *A* results in rotation of the methyl H atoms from the usual staggered position.

**The Chemistry on Diterpenoids in 1975. Part I.** E. Fujita, K. Fuji, Y. Nagao, M. Node, and M. Ochiai. *Bull. Inst. Chem. Res., Kyoto Univ.*, **54**, 197 (1976).—This is one of a series of the authors' annual reviews on diterpenoids chemistry. This review covers the literatures published between January and June 1975.

**The Antitumor and Antibacterial Activity of the *Isodon* Diterpenoids (Terpenoids 36, Biological and Physiological Activity I).** E. Fujita, K. Kaneko, S. Nakazawa, and H. Kuroda. *Chem. Pharm. Bull. (Tokyo)*, **24**, 2118 (1976).—Oridonin, lasiokaurin, enmein, enmein-3-acetate, and some related compounds, all of which have  $\alpha$ -methylene cyclopentanone function in their molecule, have been shown to have antitumor activity against Ehrlich ascites carcinoma inoculated into mice. These compounds have also indicated specific activity against gram-positive bacteria. On the other hand, oridonin dihydro-derivative, butanethiol adduct at C-17 and C-16 of oridonin, trichokaurin, and dihydroenmein show any activity against neither tumor nor bacteria. Thus, it is concluded that the  $\alpha$ -methylene-cyclopentanone system must be an important active center. Biomimetic reactions of oridonin and enmein with several thiols *etc.* support this conclusion.

**Terpenoids. 37. Hypoiodite Reactions with 6-Hydroxy-17-norkaurane- and 7-Norgibberellane-derivatives.** M. Node, H. Hori, and E. Fujita. *Chem. Pharm. Bull. (Tokyo)*, **24**, 2149 (1976).—In order to oxidize the inactive methyl group at C-19 in kaurene derivatives, the hypoiodite reaction was tried on several epimeric derivatives of *ent-kauran-6-ol*. As the result, the reaction with *kauran-6 $\beta$ -ol* derivatives which have a rigid boat form of the ring A was found to be effective for the 0-functionalization of C-19 methyl group.

In relation to the kaurene derivatives, the hypoiodite reaction on the 7-norgibberellane derivatives were also tried.

**Diterpenoids of *Isodon* and *Teucrium* Plants.** E. Fujita, Y. Nagao, and M. Node. *Heterocycles*, **5**, 793 (1976).—This review deals mainly with the authors' research works concerning isolation and characterization of new diterpenoids of *Isodon* and *Teucrium* Plants (Labiatae), their reaction and interconversion, synthesis, biosynthesis, and biological activity.

**Terpenoids. Part 39. Total Synthesis of Gibberellin A<sub>15</sub> and Gibberellin A<sub>37</sub>.** E. Fujita, M. Node, and H. Hori. *J. Chem. Soc., Perkin Trans. I*, 611 (1977).—The total synthesis of gibberellins A<sub>15</sub> and A<sub>37</sub>, in which *ent*-3 $\beta$ , 20-epoxy-3-methoxy-16 $\alpha$ -tetrahydropyran-2-yloxy-17-norkauran-6 $\alpha$ -ol was an important intermediate, is reported.

**Terpenoids. Part 40. Oxidative Rearrangement of *ent*-17-Norkauran-16-one with Thallium (III) Nitrate and Synthesis of *ent*-9(8 $\rightarrow$ 15 $\alpha$ H)*abeokaurane*.** E. Fujita and M. Ochiai. *J. Chem. Soc., Perkin Trans. I*, 1182 (1977).—Treatment of *ent*-17-norkauran-16-one with thallium trinitrate in acetic acid gave several oxidative rearrangement products. The diterpene skeleton of these rearrangement products, *ent*-9(8 $\rightarrow$ 15 $\alpha$ H)*abeokaurane*, has been synthesized.

**Biosynthesis of Natural Products. Part I. Incorporations of *ent*-16-Kaurene and *ent*-16-Kauren-15-one into Enmein and Oridonin.** T. Fujita, I. Masuda, S. Takao, and E. Fujita. *J. Chem. Soc., Perkin Trans. I*, 2098 (1976).—Incorporations of *ent*-kaur-16-ene and *ent*-kaur-16-en-15-one into enmein and oridonin by *Isodon japonicus* Hara have been demonstrated by tracer experiments with seven labelled *ent*-kaurene derivatives. Furthermore, evidence has been obtained that functionalisation of *ent*-kaur-16-ene at the allylic position C-15 proceeds through direct oxygenation.

**Terpenoids. Part 38. Ring Contraction of Kaurenolides and Related Compounds into Gibberellane-type Compounds.** M. Node, H. Hori, and E. Fujita. *J. Chem. Soc., Perkin Trans. I*, 2144 (1976).—A detailed investigation of ring B contraction has been carried out with several derivatives containing the *ent*-3 $\beta$ , 20-3, 16 $\alpha$ -dimethoxy-17-norkaurane skeleton. The 19, 6 $\beta$ -lactone 7 $\alpha$ -methanesulphonate on treatment with base and subsequent methylation gave a gibberellane aldehyde and an epimeric norkaurane derivative. The 6 $\beta$ -hydroxy-7 $\alpha$ -methanesulphonate on similar treatment gave a similar result. The 19, 6 $\alpha$ -lactone 7 $\alpha$ -methanesulphonate on treatment with potassium hydroxide in *t*-butyl alcohol-water and subsequent methylation afforded only the desired product in almost quantitative yield. The ring B contraction reaction did not proceed with the 6 $\beta$ -methanesulphonate 7 $\alpha$ -acetate. The results have been rationalized in terms of stereochemical considerations.

**Demethylation of Aliphatic Methyl Ethers with a Thiol and Boron Trifluoride.** M. Node, H. Hori, and E. Fujita. *J. Chem. Soc., Perkin Trans. I*, 2237 (1976).—Treatment of primary and secondary alkyl methyl ethers with boron trifluoride-ether complex in several thiols gave the corresponding alcohols in good yields and, in the case of secondary alkyl methyl ethers, with retention of the original stereochemistry.

**Novel Reactions of Organic Sulfur and Selenium Compounds with Thallium (III) Nitrate: Sulfoxide and Selenoxide Formation and Their**

**Pummerer-like Reaction.** Y. Nagao, M. Ochiai, K. Kaneko, A. Maeda, K. Watanabe, and E. Fujita. *Tetrahedron Lett.*, 1345 (1977).—Sulfides and selenides which have neither electron-donating nor electron-withdrawing group at the  $\alpha$ -position to the sulfur or selenium atom on treatment with thallium trinitrate (TTN) under such mild conditions as stirring at room temperature in suitable solvents gave sulfoxides and selenoxides in high yields, respectively.

The  $\beta$ -oxosulfides on treatment with TTN in methanol or its mixture with chloroform at room temperature gave the  $\beta$ -oxoacetals in satisfactory yields with the precipitation of Tl(I) nitrate.

**Acyl Migrations in Diacyl Derivatives of 2-Methylmercaptobenzimidazole. A Model of Biotin.** A. Ohno, T. Morishita, and S. Oka. *Bioorg. Chem.*, 5, 383 (1976).—Diacyl derivatives of 2-methylmercaptobenzimidazole undergo the tautomerization. Thermodynamic predominancy of one isomer over the others depends on the substituents on carbonyl groups. It has been found that electron-withdrawing substituents tend to favor N-acyl compounds, whereas electron-releasing substituents make C,C-diacyl compounds more stable. The migration has been extended to include the carboethoxy group, and the results are discussed in relation to the mechanism of biotin-dependent enzymic carboxylation.

**Reduction by a Model of NAD (P) H. XI. Stereochemistry of a Lactate Dehydrogenase-Model Reaction.** A. Ohno, T. Kimura, S. G. Kim, H. Yamamoto S. Oka, and Y. Ohnishi. *Bioorg. Chem.*, 6, 21 (1977).—Stereochemistry of the biomimetic reduction of  $\alpha$ -keto esters with NAD(P)H-model compounds has been investigated. The model compound with the *R*-configuration reduces the  $\alpha$ -keto esters to the (*R*)- $\alpha$ -hydroxy esters, whereas (*S*)- $\alpha$ -hydroxy esters are afforded by the reduction with the *S*-configurational model compounds. It has been concluded that pro-*R* and -*S* hydrogens of the model compounds with *R*- and *S*-configuration, respectively, contribute predominantly to the reduction.

**Nucleophilic Displacement Catalyzed by Transition Metal. III. Kinetic Investigation of the Cyanation of Iodobenzene Catalyzed by Palladium (II).** K. Takagi, T. Okamoto, Y. Sakakibara, A. Ohno, S. Oka, and N. Hayama. *Bull. Chem. Soc. Japan*, 49, 3177 (1976).—The nucleophilic displacement of iodobenzene with potassium cyanide was carried out in HMPA in the presence of palladium (II) acetate. The reaction obeys the following kinetics;  $d[\text{benzonitrile}]/dt = k[\text{Pd}(\text{OAc})_2]_0 (M_{\text{KCN}})^{2/3}$ . A reaction scheme composed of two cycles has been proposed: in one cycle  $\text{Pd}^0$  activates iodobenzene and in the other cycle  $\text{Pd}^{2+}$  assists the dissolution of potassium cyanide.

**Reaction of Di-*t*-butyl Thioketone with Aryllithium. Effect of Temperature and Solvent.** A. Ohno, K. Nakamura, Y. Shizume, and S. Oka. *Bull. Chem. Soc. Japan*, 50, 1003 (1977).—Di-*t*-butyl thioketone reacts with phenyllithium affording both *C*-phenylated and *S*-phenylated products. The product distribution largely depends on the reaction temperature and solvent: the lower the temperature and the

more solvated the counter cation, the larger the yield of the *S*-phenylated product. Steric effect is also important: 2,6-dimethylphenyllithium affords only *S*-arylated product. The result has been interpreted in terms of the charge-transfer-intermediate—radical-combination mechanism.

**Reduction by a Model of NAD (P) H. XIV. Mechanistic Consideration on the Role of Metal Ion.** A. Ohno, T. Kimura, H. Yamamoto, S. G. Kim, S. Oka, and Y. Ohnishi. *Bull. Chem. Soc. Japan*, **50**, 1535 (1977).—The driving force for the catalytic activity of metal ions on the reduction of  $\alpha$ -keto esters with an NAD (P) H-model compound has been discussed. The scope of the reaction and spectroscopic investigations as well as molecular orbital consideration have revealed that the transition state of the reaction consists of a ternary complex in analogy with a coenzyme-enzyme-substrate complex in an enzymic system. It is concluded that, at the transition state, one electron migrates from a model compound to a substrate through a metal ion, which is followed by the transfer of a proton.

**Reaction of *N*-Propyl-1,4-dihydronicotinamide with Ferricyanide Ion.** T. Okamoto, A. Ohno, and S. Oka. *J. Chem. Soc., Chem. Commun.*, 181 (1977).—The reaction of *N*-propyl-1, 4-dihydronicotinamide with ferricyanide ion follows a second-order rate law with Rate= $k[\text{Fe}(\text{CN})_6^{3-}][\text{PNAH}]$ . The kinetic isotope effect of the reaction has been found to be 1.68, which supports the idea that C<sub>4</sub>-H bond is loosen while one electron is transferred from PNAH to the substrate.

**Mechanism of the Chlorotris(triphenylphosphine)rhodium(I)-Catalyzed Hydrogenation of Alkenes. The Reaction of Chlorodihydridotris(triphenylphosphine)rhodium(III) with Cyclohexene.** J. Halpern, T. Okamoto, and A. Zakhariyev. *J. Molecular Catalysis*, **2**, 65 (1976).—A kinetic study of the reaction of chlorodihydridotris(triphenylphosphine)rhodium(III) with cyclohexene revealed that the equilibrium constant of the preequilibrium of the substrate complex and cyclohexene generating chlorodihydridobis(triphenylphosphine)styrenrhodium(III) and triphenylphosphine is  $(3.4 \pm 0.6) \times 10^{-4}$  and the rate constant of the insertion step is  $0.20 \pm 0.04 \text{ s}^{-1}$  at 25°C in benzene. Support for the suggestion that the rate-determining step involves Rh-H bond-breaking was provided by measurement of the kinetic isotope effect of  $k(\text{H})/k(\text{D}) = 1.15$  in chlorobenzene.

**Photocycloaddition of Thiocarbonyl Compounds to Multiple Bonds. XI. Photoaddition of Di-*t*-butyl Thioketone with Olefins.** A. Ohno, M. Uohama, K. Nakamura, and S. Oka. *Tetrahedron Lett.*, 1905 (1977).—Photochemical addition of di-*t*-butyl thioketone with certain olefins has been studied. Because of steric effect, this thioketone does not undergo the cycloaddition. Although the type of products depends on the structure of the olefin employed, it is found to be general phenomenon that photo-excited thioketone attacks C=C double bond, which is followed by 1,3- or 1,5-hydrogen atom migration to give a di-*t*-butylmethyl group.

**Reduction by a Model of NAD (P) H. XII. Effect of Substituents on the Stereospecificity of the Reaction.** A. Ohno, H. Yamamoto, T. Kimura, S. Oka, and Y. Ohnishi. *Tetrahedron Lett.*, 4585 (1977).—The nature of the 3-substituent on 1-p-ropyl-1,4-dihydropyridine influences the optical yield of the product in the reduction of benzoylformate. The optical yield is the highest with 3-N-methyl-carbamoyl group and the lowest with 3-menthoxy-carbonyl group. 3-Menthyl-methyl-carbonyl group sits between of them. The result has been interpreted in terms of the mobility of a proton next to the carbonyl group. That is, enolization and chelation of the carbonyl group on to a metal ion is an important factor.

**Reaction of Alkyl Halides with Mercury (II) Salts in Tetrahydrofuran. A Facile Preparation of 4-Alkoxybutyl Acetates and Chlorides.** N. Watanabe, S. Uemura, and M. Okano. *Bull. Chem. Soc. Japan*, **49**, 2500 (1976).—The reaction of primary and secondary alkyl iodides and bromides with  $\text{Hg}(\text{OAc})_2$  and  $\text{HgCl}_2$  in tetrahydrofuran (THF) affords the THF-incorporated compounds (1),  $\text{RO}(\text{CH}_2)_4\text{X}$  [ $\text{X}=\text{OAc}$  and  $\text{Cl}$ , respectively], in good yields. When  $\text{HgBr}_2$  and aqueous or alcoholic  $\text{Hg}(\text{ClO}_4)_2$  were used as mercury (II) salts, the yields of 1 ( $\text{X}=\text{Br}$ ,  $\text{OH}$ , and  $\text{OR}'$ ) were low. Similar treatment with  $\text{HgI}_2$  gave scarcely any 1. A reaction scheme which involves *O*-alkyltetrahydrofuranium ion as the intermediate is proposed for the formation of 1.

**The Reaction of Arylthallium (III) Compounds with Metal Nitrite. Synthesis of Nitroarenes.** S. Uemura, A. Toshimitsu, and M. Okano. *Bull. Chem. Soc. Japan*, **49**, 2582 (1976).—Arylthallium (III) compounds react smoothly with various metal nitrites such as  $\text{NaNO}_2$ ,  $\text{KNO}_2$ , and  $\text{AgNO}_2$  in trifluoroacetic acid to give nitroarenes in good yields. It has been clarified that the reaction proceeds through substitution of thallium moiety by nitroso group at the (*ipso*) position where thallium was attached previously to aromatic ring to give nitrosoarenes, followed by their oxidation to nitroarenes.

**Preparation of Some Alkylthallium (III) Dichlorides and Their Reactions with Potassium and Copper Halides.** S. Uemura, A. Toshimitsu, and M. Okano. *Bull. Chem. Soc. Japan*, **49**, 2762 (1976).—A simple synthesis is given for the stable monoalkylthallium (III) dichloride,  $\text{C}_6\text{H}_5\text{CH}(\text{OR})\text{CH}_2\text{TlCl}_2$  (1) from the corresponding diacetate (2) and potassium chloride in methanol or acetonitrile. 1 ( $\text{R}=\text{Me}$ ) reacts slowly with potassium and copper (I) halides to give mainly  $\alpha$ -methoxystyrene and  $\text{C}_6\text{H}_5\text{CH}(\text{OMe})\text{CH}_2\text{X}$  ( $\text{X}=\text{Cl}$ ,  $\text{Br}$ ,  $\text{I}$ ), respectively. It is concluded that 1 ( $\text{R}=\text{Me}$ ) is less susceptible than 2 ( $\text{R}=\text{Me}$ ) to  $\text{S}_{\text{N}}1$ ,  $\text{S}_{\text{N}}2$ , and  $\text{S}_{\text{N}}\text{i}$  reactions.

**Oxidation of Olefins with Thallium (III) Acetate in Diols.** S. Uemura, H. Miyoshi, A. Toshimitsu, and M. Okano. *Bull. Chem. Soc. Japan*, **49**, 3285 (1976).—The oxidation of styrene,  $\alpha$ - and  $\beta$ -methylstyrene, and 1-octene with thallium (III) acetate in diols,  $\text{HO}(\text{CH}_2)_n\text{OH}$  ( $n=2, 3$ , and  $4$ ), has been investigated. From styrene the derivatives of 1,3-dioxolane, 1,3-dioxane, and 1,3-dioxepane were mainly obtained for  $n=2, 3$ , and  $4$  respectively, while the reaction of 1-octene in 1,2-ethanediol afforded

1-acetoxy-2-(2-hydroxyethoxy)octane as the main product. A new alkoxythallate of styrene,  $C_6H_5CH(OCH_2CH_2OH)CH_2Tl(OAc)_2$ , has been isolated under milder conditions.

**The Efficient Oxidation of Thiols to Disulfides with Thallium (III) Acetate.** S. Uemura, S. Tanaka, and M. Okano. *Bull. Chem. Soc. Japan*, **50**, 220 (1977).—The treatment of various kinds of alkane- and arenethiols with thallium (III) acetate in chloroform at 20–30°C readily affords the corresponding disulfides almost quantitatively, without affecting other functional groups, such as the hydroxyl, amino, and carboxyl in the thiols. Under similar conditions, the reaction of thiobenzoic *S*-acid with thallium(III) acetate gives thallium (III) thiobenzoate, while that of thioacetic *S*-acid yields diacetyl disulfide and thallium (I) thioacetate.

**The Reactions of Carbonimidoyl Dichlorides with Metal Thioacetates, Acetates, Thiocyanates, and Selenocyanate.** S. Tanaka, S. Uemura, and M. Okano. *Bull. Chem. Soc. Japan*, **50**, 722 (1977).—The reactions of carbonimidoyl dichlorides with potassium thioacetate and thiocyanate in tetrahydrofuran afford the corresponding isothiocyanates. Similarly, the reaction with potassium selenocyanate gives isoselenocyanates. Thallium (I) acetate reacts with phenylcarbonimidoyl dichloride with greater facility than potassium acetate to give a mixture of phenyl isocyanate and acetanilide in which the latter is predominant. A displacement of one chlorine atom in the carbonimidoyl dichlorides by a SAC, OAc, SCN, or SeCN group, followed by elimination of AcCl or CNCl, has been proposed as a reasonable reaction path.

**The Transannular Cyclization and Hydrogen Shift in the Chlorination of 1,5-Cyclooctadiene and *cis*-Cyclooctene with Antimony (V) Chloride.** S. Uemura, A. Onoe, and M. Okano. *Bull. Chem. Soc. Japan*, **50**, 1078 (1977).—The slow addition of  $SbCl_5$  to a  $CCl_4$  solution of 1,5-cyclooctadiene or *cis*-cyclooctene gives an isomeric mixture of *endo*- and *exo*-2, *anti*-8-dichlorobicyclo[3.2.1]-octanes (1 and 2) or an isomeric mixture of *trans*- and *cis*-1,4-dichlorocyclooctanes (12 and 13) respectively in a good yield. The former reaction involves the transannular cyclization, while the latter is accompanied by the transannular hydrogen shift. The addition of 1,5-cyclooctadiene to a  $CCl_4$  solution of  $SbCl_5$  (reverse addition) affords *endo*-2,6- and *endo*, *exo*-2,6- dichlorobicyclo [3.3.0]octanes (6 and 7) as additional products, besides 1 and 2. In the case of *cis*-cyclooctene, however, a reverse addition produces only chlorocyclooctane. It has been revealed that a mixture of 6 and 7 is readily isomerized to a mixture of 1 and 2 by the interaction with  $SbCl_5$ . The 1,4-chlorination of *cis*-cyclooctene which gives 12 and 13 also occurs with  $VCl_4$ ,  $SeCl_4$ ,  $PhICl_2$ , and  $PCl_5$  although the selectivity and the yield are low compared to the case of  $SbCl_5$ .

**A Three-Component Reaction of Isocyanides with Halogens and Cyclic Ethers.** T. Yamazaki, Y. Wada, S. Tanimoto, and M. Okano. *Bull. Chem. Soc. Japan*, **50**, 1094 (1977).—In the presence of Lewis-acid catalyst, such as  $HgCl_2$  or  $ZnCl_2$ , cyclohexyl isocyanide reacted with chlorine and tetrahydrofuran to give, after

hydrolysis, 4-chlorobutyl cyclohexylcarbamate in a fair yield. When one of the reactants was replaced by another isocyanide, bromine, or another cyclic ether, the reactions proceeded similarly, but the corresponding carbamate yields were rather poor.

**Dichlorocarbene Formation from Thallium (I) Butanethiolate and Chloroform.** S. Uemura, S. Tanaka, and M. Okano. *Bull. Inst. Chem. Res., Kyoto Univ.*, 55, 273 (1977).—The reactions of cyclohexene and  $\alpha$ -methylstyrene with thallium (I) butanethiolate (TIS-*n*-Bu) in chloroform at a refluxing temperature for 3 h gave the corresponding *gem*-dichlorocyclopropane derivatives in 11% and 22% yield respectively. Other thiolates of thallium (I) such as TISEt, TIS-*t*-Bu, and TISPh, and other metal butanethiolates such as Pb(S-*n*-Bu)<sub>2</sub> and NaS-*n*-Bu showed lower reactivity than TIS-*n*-Bu for the generation of dichlorocarbene.

**Synthesis of 2-Ethoxy-1,3-oxathiolane and 2-Ethoxy-1,3-dithiolane and Their Some Reactions.** S. Tanimoto, T. Miyake, and M. Okano. *Bull. Inst. Chem. Res., Kyoto Univ.*, 55, 276 (1977).—The synthesis of 2-ethoxy-1,3-oxathiolane (II) and 2-ethoxy-1,3-dithiolane (III) from ethyl orthoformate by transesterification reaction was described. The stability toward a trace amount of aqueous acid was found to decrease in the order: 2-ethoxy-1,3-dioxolane (I) > II > III, and the disproportionation products (or its hydrolysis product) were isolated from the reaction with II or III. In the reaction with *n*-BuMgBr, I gave 1-ethoxy-1-[2-(hydroxy)ethoxy]pentane and 2-butyl-1,3-dioxolane, and II gave 2-butyl-1,3-oxathiolane. On the other hand, in the reaction with *n*-BuLi, both I and II afforded 5-nonanol and 5-butyl-5-nonanol, and III afforded two corresponding thiols. Probable pathways for these transformation are briefly considered.

**Oxyselenation of Olefins by the Use of Aryl or Alkyl Selenocyanates and Copper or Nickel Halides.** A. Toshimitsu, S. Uemura, and M. Okano. *J. Chem. Soc., Chem. Comm.*, 166 (1977).—Reaction of olefins with aryl or alkyl selenocyanates in alcohol, water, or acetic acid in the presence of copper or nickel (II) halides produces the corresponding  $\beta$ -oxy selenides in high yields.

**Chlorination and Chloriodination of Acetylenes with Copper (II) Chloride.** S. Uemura, H. Okazaki, A. Onoe, and M. Okano. *J. Chem. Soc., Perkin Trans. I.* 676 (1977).—Reactions of acetylenes (RC $\equiv$ CR'; R and/or R'=H, alkyl, or phenyl) (1), with copper (II) chloride-lithium chloride in acetonitrile give the corresponding *E*-dichloroalkenes in good yields except in the case of (1; R=Ph, R'=Bu<sup>t</sup>) where the *Z*-product is favored. Reactions with copper (II) chloride-iodine or -potassium iodide proceed more smoothly to afford, completely regiospecifically and highly stereospecifically, *E*-chloroiodoalkenes in high yields. Reactions with iodine chloride also give the same compounds, but the yield and *E*-stereospecificity are low in comparison with those in the copper (II) chloride-iodine case. An open vinyl cation intermediate in which copper (I) co-ordinates weakly with both the double bond and the chlorine atom attached to carbon is postulated for chlorination,



and a cyclic iodonium ion intermediate is proposed for chloriodination.

**Selective Diarylmethane Formation in the Reaction of Iron (III) Perchlorate with Alkylbenzenes.** S. Uemura, S. Tanaka, and M. Okano. *J. Chem. Soc., Perkin Trans. I*, 1966 (1976).—Treatment of alkylbenzenes with iron (III) perchlorate in acetic acid affords diarylmethanes selectively in good yields; the formation of biaryls reported in previous studies with iron (III) chloride was not observed. Reactions with other iron (III) salts in the presence of perchloric acid proceed similarly. The reaction is interpreted in terms of formation of a benzylic cation, followed by its electrophilic attack on another alkylbenzene molecule.

**A Facile Preparation of Aromatic Carboxylic Acid Esters by the Reaction of 1,3-Butadienylamine and 1,3-Butadienyl Ether with Acetylene Carboxylic Acid Esters.** S. Tanimoto, Y. Matsumura, T. Sugimoto, and M. Okano. *Tetrahedron Lett.*, 2899 (1977).—This communication deals with the results that the substituted 1,3-butadienes, such as N,N-diethyl-1,3-butadienylamine, 4-(1,3-butadienyl)morpholine and 1,3-butadienyl ethyl ether, reacted readily with acetylene carboxylic acid esters to afford aromatic carboxylic acid esters in good yields.

**Reaction of Aryne with N,N-Diethyl-1,3-Butadienylamine.** S. Tanimoto. *Tetrahedron Lett.*, 2903 (1977).—This communication has described the Diels-Alder reaction of N,N-diethyl-1,3-butadienylamine with the aryne generated by the action of a strong base on halobenzene or halonaphthalene. The reaction can serve as a general method to prepare naphthalene or phenanthrene from halobenzene or halonaphthalene in both a one-step manner and a desirable yield.

## Polymer Chemistry

**Polymer Separation and Characterization by Thin-Layer Chromatography.** H. Inagaki. *Advances in Polymer Science*, **24**, 190 (1977).—This article is a review describing recent advances in application of thin-layer chromatography (TLC) to polymer separation and characterization. Chapter II presents the theoretical backgrounds including different separation mechanisms applicable to TLC. Possibilities of determining compositional heterogeneities of different copolymers are discussed in chapter III; while those of distinguishing chain architecture of different types of polymers in chapter IV. Chapter V deals with TLC separations by solubility-controlled mechanism which lead to polymer fractionation according to the molecular weight. Some experimental problems experienced by our research group are described in chapter VI.

**Particle Scattering Function for Spherical Block Copolymer Micelles.** T. Tanaka, T. Kotaka, and H. Inagaki. *Bull. Inst. Chem. Res., Kyoto Univ.*, **55**, 206 (1977).—The Debye particle scattering function  $P$  was calculated on the "three-phase model" representing a spherical multimolecular micelle formed by an AB diblock copolymer. The model consists of the three phases, *i.e.*, a pure B phase forming the

spherical "core", an A-B intermixing phase forming the "shell" in which the A-B junctions are located, and a pure A phase forming the "fringe" surrounding the shell and the core. The A chains were assumed to obey the statistics of the random-flight chain with one end (*i.e.*, the junction) bound near the impermeable surface (of the B core). The calculations showed that the  $P^{-1}$  vs  $C \sin^2(\theta/2)$  curve with the constant C so chosen as to give the initial slope of 1/3 increases with increasing angle much more rapidly than that for the linear chain, but less rapidly than that for the uniform-density model, essentially in agreement with observations. The method to analyze, on the basis of the model, experimental data obtained from the core-component-invisible micelle systems was discussed. It was shown that new information about the micelle morphology is obtainable. Above all, the extent of expansion of the A chains in the radial direction could be determined with little (theoretical) ambiguity.

**Conformation of Block Copolymers in Dilute Solution. Monte Carlo Calculations and Light-Scattering Studies on Diblock Copolymer Systems.**

T. Tanaka, T. Kotaka, and H. Inagaki. *Macromolecules*, **9**, 561 (1976).—Conformational properties of AB-diblock copolymers in dilute solution were examined by two different methods. One is computer simulation on a self-avoiding type lattice-walk model. The other is light-scattering measurements made with solvents having zero refractive index increments for one of the two blocks, say B. Existing light-scattering data of this kind as well as ours were analyzed taking the small visibility of the B block into account. Both methods led to a common conclusion that the mean-square radii of gyration of the individual blocks are almost the same as those of the homopolymers equivalent to the respective blocks, in any case. On the other hand, the computer simulation indicated that the mean-square distance between the centers of mass of the two blocks increases noticeably with increasing A-B repulsive interactions, making the conformation of the overall chain as well as those of the individual blocks more asymmetrical. It was indicated that such an effect of the heterocontact interactions would be less significant as the individual blocks become more expanded due to the excluded volume effects within the respective blocks (*i.e.*, with the solvent quality becoming better toward the parent homopolymers). A possible range over which this center-to-center distance may vary was suggested.

**Conformation of Flexible Polymers Near an Impermeable Surface.**

T. Tanaka. *Macromolecules*, **10**, 51 (1977).—Statistics on a random-flight chain which is bound on or near an impermeable, noninteracting planar surface with one end or both ends were developed. Probability densities of finding a given number of segments at respectively specified locations were obtained as functions of the location(s) of end segment(s). From these functions some new information about the conformational properties of flexible polymers near the surface was derived such as overall density distribution of segments and moments of segment distribution about the end segment and about the center of mass, all as functions of the location(s) of end segment(s). As for the so-called "tail" chain, the first-order coefficient of the perturbation theory of excluded-volume effects concerning the mean-square end-to-end distance was also derived.

**Short-Range Order in Deformed Polymer Networks.** T. Tanaka and G. Allen. *Macromolecules*, **10**, 426 (1977).—Mechanism of short-range ordering in deformed polymer networks was discussed from the point of view of the lattice theory of DiMarzio. It was shown that on stretching a network, the segments tend to order along the stretching direction to decrease the mutual interference between them, *i.e.*, the volume effects. The extent of ordering was estimated using a simple set of self-consistent models, leading to the indication that the extra amount of segment orientation would be of the same order of magnitude as the amount which the system would show in the absence of the volume effects. The effects resulted in a negative contribution to the stress-strain relation, which is much larger than DiMarzio's estimation.

**Separation and Characterization of Block and Graft Copolymers by Thin-Layer Chromatography.** H. Inagaki, T. Kotaka, and Tae-Ik Min. *Pure and Appl. Chem.*, **46**, 61 (1976).—Feasibilities of thin-layer chromatography (TLC) and its combination with gel permeation chromatography in characterization of block and graft copolymers are discussed. The simplest application of TLC is to test the purity of block and graft samples having been subjected to purification treatment. TLC allows further to determine the compositional heterogeneity of block copolymers without interference of molecular weight, and to distinguish block samples by the difference in block sequence even on the same composition level. The latter applicability is illustrated for styrene-butadiene copolymers with different chain architecture. Finally two applications of TLC as a tool for characterization of graft systems are described: one is to isolate side-chain polymers truly grafted on mother polymer chains, and the other to isolate true graft copolymers from reaction products.

**Determination of Functionality Distributions in Telechelic Prepolymers by Thin-Layer Chromatography.** T.I. Min, T. Miyamoto, and H. Inagaki. *Rubber Chem. and Technol.*, **50**, 63 (1977).—Functionality distributions of telechelic prepolymers have been determined by thin layer chromatography (TLC). Commercially available 1,2-polybutadienes having either carboxyl or hydroxyl groups were examined. TLC with p-xylene as the developer made it possible to separate the sample into a nonfunctional component and a mixture of mono- and difunctional components. Complete separation of the sample into the three components was achieved by selecting the developer and development procedure appropriately. Quantification of the chromatograms was performed successfully in a TLC apparatus equipped with a flame ionization detector. A simple method for the determination of the functionality distribution was proposed.

**Nonlinear Viscoelasticity of Polystyrene Solutions. III. Stress Development at the Start of Steady Shear Flow and Experimental Check of Some Constitutive Models.** K. Osaki, S. Ohta, M. Fukuda, and M. Kurata. *J. Polym. Sci., Polym. Phys. Ed.*, **14**, 1701 (1976).—The development of the shear stress at the start of shear flow at constant rate of shear  $\dot{\epsilon}$  was measured for polystyrene solutions in diethyl phthalate with a cone-and-plate rheometer. Ranges of molecular weight

$M$  and concentration  $c$  were  $3.10 \times 10^6 - 7.62 \pm 10^6$  and  $0.112 - 0.329$  g/cm<sup>3</sup>, respectively. The shear stress as a function of time  $t$  exhibited a marked maximum at large  $\kappa$  when either  $M$  or  $c$  was relatively low. When  $M$  and  $c$  were high, the maximum was broad and low. In a few extreme cases no maximum was observed in the range of  $\kappa$  studied. The constitutive model of Bernstein, Kearsley, and Zapas could describe approximately the shear stresses at a sudden start and on cessation of steady shear flow with a memory function evaluated from the strain-dependent relaxation modulus. The strain dependence of the memory function for solutions of low  $M$  or  $c$  was approximately expressed as  $\exp\{-\alpha|s|\}$  where  $\alpha$  is a constant (ca. 0.37) and  $|s|$  is the absolute value of shear strain. When  $M$  and  $c$  were high, the strain dependence was found to be more diffuse and to require several terms if approximated by exponential functions of  $|s|$ . The Lodge model based on a strain-rate dependent relaxation spectrum was not able to describe the strain-dependent relaxation modulus as well as the interrelation between shear stresses at a sudden start and a cessation of steady shear flow.

**Linear Viscoelastic Relation Concerning Shear Stresses at the Start and Cessation of Steady Shear Flow.** K. Osaki, A. Murai, N. Bessho, and B.S. Kim. *Nippon Reorosi Gakkaishi (J. Soc. Rheology, Japan)*, 4, 166 (1976), in Japanese.—This paper deals with the linear viscoelastic relations for transient shear stresses at the start and cessation of steady shear flow. Viscosity growth function  $\eta(t)$  and viscosity decay function  $\bar{\eta}(t)$  were defined as the limiting values at vanishing rate of shear, of the ratios of shear stresses to the rate of shear at the start and cessation, respectively, of steady shear flow. A short review was given for exact interrelations among  $\bar{\eta}(t)$ ,  $\eta(t)$ , and other linear viscoelastic functions. Approximation equations for evaluating various functions from the relaxation modulus could be easily transformed into equations for evaluating various functions from  $\eta(t)$ . Proposed approximation formulae for complex viscosity and relaxation spectrum proved usable when examined numerically in the cases of wedge- and box-type relaxation spectra. The approximation formulae for the relaxation spectrum may be employed for determining the rate-dependent relaxation spectrum of nonlinear viscoelasticity.

**Flow Birefringence of Polymer Solutions in Time-Dependent Shear Flow. I. Measurements on Sudden Application of Torsional Shear.** N. Bessho, K. Osaki, and M. Kurata. *Nippon Reorosi Gakkaishi (J. Soc. Rheology, Japan)*, 5, 68 (1977), in Japanese.—Flow birefringence was measured for a 20% polystyrene solution in chlorinated biphenyl on sudden application of shear strain. The sample was torsionally sheared between two parallel glass plates and the time-dependent birefringence was measured with a light beam directed perpendicularly to the shearing plane. Measurements were performed over the range of shear  $0.8 \leq \dot{\gamma} \leq 5.4$  and the range of time  $5s \leq t \leq 300s$ . The normal stress difference  $\sigma_{11} - \sigma_{33}$  evaluated from the birefringence with the use of stress-optical law was slightly smaller than the product  $\dot{\gamma}\sigma_{12}$  over the whole range of measurements. Here the subscript 1 denotes the direction of flow, 2 the direction perpendicular to the shearing plane, and 3 the neutral direction. According to the Lodge theory that  $\dot{\gamma}\sigma_{12}$  should be equal to the first normal stress difference  $\sigma_{11} - \sigma_{22}$ , we deduced from the experimental results that the second normal

stress difference  $\sigma_{22} - \sigma_{33}$  was negative and its magnitude was less than 10% of  $\sigma_{11} - \sigma_{22}$ .

**Randomly Branched Polymers. I. Hydrodynamic Properties.** M. Kurata, M. Abe, M. Iwama, and M. Matsushima. *Rubber Chem. and Technol.*, **49**, 1276 (1976).—Reprinted from *Polymer Journal* **3**, 729 (1972); see also this *Bulletin*, **51**, 402 (1973).

**Randomly Branched Polymers. II. Computer Analysis of Gel-Permeation Chromatograms.** M. Kurata, H. Okamoto, M. Iwama, M. Abe, and T. Homma. *Rubber Chem. and Technol.*, **49**, 1290 (1976).—Reprinted from *Polymer Journal*, **3**, 739 (1972); see also this *Bulletin*, **51**, 402 (1973).

**The Crystal Structure of Polyethylene at 4.5°K.** A. Kawaguchi, R. Matsui, and K. Kobayashi. *Bull. Inst. Chem. Res., Kyoto Univ.*, **55**, 217 (1977).—A cryostat for X-ray diffraction work with a diffractometer was constructed. This apparatus was utilized for the crystal structure analysis of polyethylene. Polyethylene was crystallized at 129°C and its X-ray measurements were carried out at 4.5°K. The crystal parameters were refined by the least squares method. The cell dimensions are:  $a = 7.12_8 \text{ \AA}$ ,  $b = 4.85_2 \text{ \AA}$ ,  $c = 2.55_5 \text{ \AA}$ . The setting angle is  $45.5 \pm 3^\circ$ .

**An Optical Study on Shear-Induced Crystallization of Polymers.** K. Nogami, S. Murakami, K. Katayama, and K. Kobayashi. *Bull. Inst. Chem. Res., Kyoto Univ.*, **55**, 227 (1977).—The process of shear-induced crystallization of some polymers was examined by means of an X-ray TV system and the polarized light scattering method. The process of shear-induced crystallization under low stress was proved to be essentially the same as that of spherulitic growth. Under high shear stress, light scattering was observed as a premonitory sign of crystallization before X-ray crystalline reflections start to appear. The strong scattering on the equator in the Vv light scattering pattern before the crystallization point indicates that many elongated bodies, which are precursors of the row structure, have occupied a large portion of the specimen at the crystallization point. It is inferred from the results that, in the course of shear-induced crystallization under high stress, there may exist a mesomorphic state during transformation from the amorphous to the crystalline state.

**Construction of Image Processing Systems and Application to the Random Noise Removal in Electron Micrographs.** M. Tsuji, S. Isoda, M. Ohara, K. Katayama, and K. Kobayashi. *Bull. Inst. Chem. Res., Kyoto Univ.*, **55**, 237 (1977).—Computer and optical image processing systems were constructed to obtain high resolution images from electron micrographs. It seems that the main source of image degradation is the photographic graininess in electron-microscopic films. Spatial frequency filtering and linear integration are applied to the removal of random noises caused by the graininess of images. Signal-to-noise ratio is increased extremely in either processing. In particular, if both the periodic and the large scale irregular structures are required to be kept in processed images, spatial frequency filtering will be useful for the improvement in the signal-to-noise ratio.

**Phase Structure and Molecular Mobility of Polyethylene Fibers by Broad-Line NMR Spectroscopy.** S.-H. Hyon, F. Horii, and R. Kitamaru. *Bull. Inst. Chem. Res., Kyoto Univ.*, **55**, 248 (1977).—The phase structure of polyethylene filaments with different draw ratios is studied by broad-line NMR spectroscopy. The broad-line spectrum is analyzed in terms of contributions from three regions; a crystalline region (broad component), a noncrystalline region that has a liquidlike character (narrow component), and an intermediate region (medium component).

It is found that the mass fraction and molecular mobility of each region depend greatly on the degree of drawing.

- (1) The broad and medium components increase with decreasing narrow component as the degree of drawing increases.
- (2) The molecular mobility of the medium component decreases greatly with increasing degree of drawing.
- (3) The narrow component diminishes but a minor component with liquidlike mobility remains even at high degrees of drawing.

Such a change in the three components of spectra upon drawing is also reflected in the swelling effects in non-protonated solvent such as  $\text{CCl}_4$ . The results for such three components are discussed in relation to the morphological phase structure of samples.

**Highly Accessible or Decrystallized Cotton by Chemical Methods.** W. Tsuji, A. Hirai, and M. Hosono. *J. Appl. Polym. Sci.*, **20**, 2837 (1976).—To obtain highly accessible cotton by cyanoethylation with acrylonitrile after pretreatment with swelling agents, the effect of various swelling agents was examined. Swelling agents such as lithium hydroxide, sodium hydroxide, potassium hydroxide, ethylamine, triethylamine, ethylenediamine, piperazine, benzyltrimethylammonium hydroxide (BTMOH), urea, dimethyl sulfoxide, dimethylformamide, zinc chloride, and liquid ammonia were examined. It was found that the sodium hydroxide pretreatment or the dual pretreatment with either potassium hydroxide, ethylenediamine, or BTMOH, and sodium hydroxide prior to acrylonitrile treatment gave modified cottons having moisture regain as high as 14%. In such cases, maximum values of moisture regain were observed at the degrees of cyanoethylation of 5–8%.

**Structure of Decrystallized Cotton in Fabrics Prepared by Alkali and Acrylonitrile Treatments.** A. Hirai, W. Tsuji, R. Kitamaru, and M. Hosono. *J. Appl. Polym. Sci.*, **20**, 3365 (1976).—The crystalline structure of decrystallized cotton, prepared by partial cyanoethylation with the use of sodium hydroxide aqueous solution and acrylonitrile, was examined by X-ray and IR data, in connection with such fabric properties as moisture regain. It was found that the moisture regain of the cotton fabric first increased, passed through a maximum at about 6 mole-% of cyanoethylation, and then slightly decreased with increasing degree of cyanoethylation. The increase of moisture regain in the region of the lower degree of cyanoethylation was well related to the decrease in the crystallinity of cotton. The X-ray diffraction studies revealed that the distension and disorder of the unit cell occurred primarily in the direction perpendicular to the (101) crystal plane as cyanoethylation proceeded.

**Reaction of Poly (vinyl Alcohol) with Pentavalent Vanadium Ion.** Y. Ikada, Y. Nishizaki, Y. Uyama, T. Kawahara, and I. Sakurada. *J. Polym. Sci., Polym. Chem. Ed.*, **14**, 2251 (1976).—The reaction of poly(vinyl alcohol) (PVAL) with V(V), *i.e.*, pentavalent vanadium ion, was studied in aqueous H<sub>2</sub>SO<sub>4</sub> medium. The viscosity change of reaction mixture with time showed a peculiar feature owing to formation of labile complex between V(V) and PVAL and the subsequent decomposition of the complex. On the other hand, the change of viscosity disappeared when NaOH was added during the reaction to neutralize H<sub>2</sub>SO<sub>4</sub> in the reaction mixture. Under a suitable condition, the reaction mixture set to a gel as a result of complex formation. It appeared that reactive sites in PVAL responsive to complexing with V(V) were 1,2-glycol unit and 1,2-ketoalcohol unit resulting from the oxidation of 1,2-glycol by V(V). The rate of oxidation was increased with increasing H<sub>2</sub>SO<sub>4</sub> concentration. The main-chain scission of PVAL took place to an insignificant extent, unless the reaction condition was severe. Based on the results obtained a reaction mechanism has been proposed.

**Reaction of Poly(vinyl Alcohol) with Tetravalent Ceric Ion.** Y. Ikada, Y. Nishizaki, H. Iwata, and I. Sakurada. *J. Polym. Sci., Polym. Chem. Ed.*, **15**, 451 (1977).—Poly(vinyl alcohol) (PVAL) was oxidized by ceric ion, Ce(IV), in aqueous HNO<sub>3</sub> medium at different temperatures and found to be degraded as a result of selective cleavage of the 1,2-glycol unit existing in PVAL. The rate of oxidation increased with increasing temperature. The aldehyde groups formed at the ends of the degraded polymer upon oxidation were relatively stable at 0°C. With rise of temperature, the aldehyde groups reacted either with excess of Ce(IV) to carboxylic acids or with hydroxyl groups of PVAL molecules to give acetal linkage. When the acetalization predominated over the oxidation to carboxyl group, gelation of the reaction mixture was observed. Based on these results, a plausible mechanism of oxidation of PVAL with Ce(IV) and the subsequent reactions is discussed.

**Proton Magnetic Resonance Spectrum of Linear Polyethylene in the Melt.** F. Horii, R. Kitamaru, and T. Suzuki. *J. Polym. Sci., Polym. Lett. Ed.*, **15**, 65 (1977).—The NMR absorption spectrum of polyethylene in the melt is not described by a single Lorentzian line shape. This fact was argued by some investigators as to indicate that the molten state of the polymer was not homogeneous but a heterogeneity such as bundles of parallel chain elements existed. However, in this paper the origin of the non-single Lorentzian line is sought in another way, considering the distribution of NMR correlation times  $\tau_c$  owing to a variety of segmental motions of chains.

When a rectangular distribution was assumed for  $\ln \tau_c$ , the theoretical spectrum was in good accord with the observed spectrum for many samples with different molecular weights. Thus it is concluded that the non-Lorentzian line shape of molten polyethylene can be explained by the distribution of correlation times. It does not imply that the structure is not homogeneous but indicates a variety of segmental motion for molecular chains of the polymer.

**Proton Magnetic Resonance Studies of the Phase Structure of Bulk-Crystallized Linear Polyethylene.** R. Kitamaru, F. Horii, and S.-H. Hyon. *J. Polym. Sci., Polym. Phys. Ed.*, 15, 821 (1977).—The broad-line proton NMR spectra of melt-crystallized samples of polyethylene covering a very wide range in molecular weight have been analyzed in terms of contributions from three components: 1) a crystalline region with crystals of orthorhombic form; 2) a noncrystalline region with liquid-like character which produces a Lorentzian contribution to the spectrum; and 3) an intermediate region in which the rotation of methylene groups about C-C bonds is partly hindered. The relative mass fractions as well as the character of these components depend greatly on the molecular weight. Samples of low molecular weight (e.g.,  $\leq 30,000$ ) are predominantly composed of lamellar crystalline regions with a minor amount of interfacial regions and no liquid-like interzonal regions. As the molecular weight increases beyond 45,000, an interzonal region with a liquid-like character associated with a higher molecular mobility is produced. Above a molecular weight of 100,000, this liquid-like character becomes pronounced with an increase in molecular mobility in the interfacial region.

**The Structure of Polymers in the Amorphous State.** K. Kaji. *Kobunshi (High Polymers, Japan)*, 25, 477 (1976), in Japanese.—Recent progress in the structure of polymers in the amorphous state was reviewed. The neutron small-angle scattering gives the radius of gyration of a molecule in the bulk amorphous state, which was found to be equal to the value for a random coil chain in  $\theta$ -solvent. Radial distribution analysis by electron diffraction method shows that there are no short-range orders in the amorphous state. The density fluctuation, which might be expected for the module structure observed by electron microscopy, could not be seen by the small-angle X-ray scattering. Most results support the Flory's random coil model for the amorphous state.

**Ionic Bonding between Acetalized Poly(vinyl Alcohol) with Diethoxyethyltrimethylammonium and Sulfated Poly(vinyl Alcohol).** M. Hosono, S. Sugii, O. Kusudo, and W. Tsuji. *Kobunshi Ronbunshu*, 33, 509 (1976), in Japanese.—The formation of complex between partially acetalized poly(vinyl alcohol) with diethoxyethyltrimethylammonium (I) and partially sulfated poly(vinyl alcohol) (II) was studied mainly by nephelometry. (1) The aqueous solutions of I and II were mixed and the turbidity was measured as a function of the mixing ratio. Generally a clear maximum (or minimum when the polyion complexes precipitated) of turbidity was observed for the stoichiometric equivalent mixture of I and II, independent of the stirring condition and the pH of the solutions. (2) It was found by the analysis of N and S contents that the polyion complex produced at the maximum (or minimum) turbidity was composed of the equivalent mixture of I and II. (3) The complex formation was investigated also in the presence of salts (NaCl, CaCl<sub>2</sub>) under stirring. The turbidity generally increased sharply with increasing the salt concentration to a certain point, then decreased eventually to zero regardless of the mixing ratio. A mechanism of the complex formation in the presence of salts was proposed. (4) Some organic solvents such as dimethylsulfoxide showed retarding effects on the



complex formation.

**Preparation of Hydrogels by Radiation Technique.** Y. Ikata, T. Mita, F. Horii, I. Sakurada, and M. Hatada. *Radiat. Phys. and Chem.*, **9**, 633 (1977).—Moderately concentrated, aqueous solutions of poly(vinyl alcohol) (PVA), poly(ethylene oxide), polyacrylamide, polyvinylpyrrolidone, and methyl cellulose were cast on a glass plate and irradiated with electron beams to yield crosslinked hydrogels. Irradiation was carried out also for water-swollen films of PVA. In all cases, no attempt was made to expel air from the polymer-water mixture to be irradiated, since the hydrogels were readily formed by placing a glass plate or a plastics film on the mixture. The measurement of tensile properties of the hydrogels revealed that the hydrogel from PVA, especially prepared by irradiation of water-swollen films, gave the highest tensile strength among the hydrogels. The swelling of once dried PVA hydrogels was recovered almost to the initial swelling state when boiled in water.

### Biochemistry

**Further Characterization of Glutaminase Isozymes from *Pseudomonas aeruginosa*.** M. Ohshima, T. Yamamoto, and K. Soda. *Agr. Biol. Chem.*, **40**, 2251 (1976).—(1) Both glutaminases A and B of *Pseudomonas aeruginosa* are inactivated by urea and guanidine hydrochloride, and the activities are partially restored by removal of the denaturants, while sodium lauryl sulfate denatured irreversibly the isozymes. (2) Glutaminase A consists of 4 identical subunits (mol. wt., 35,000) and B is composed of one polypeptide chain (mol. wt., 67,000). (3) Glutaminase A, which catalyzes the hydrolysis and also the hydroxylaminolysis of L and D isomers of glutamine and asparagine, does not act on  $\gamma$ -N-substituted glutamine *e.g.*,  $\gamma$ -glutamylhydrazide. Some L- and D- $\gamma$ -glutamyl derivatives, *e.g.*, L- and D- $\gamma$ -glutamylmethylester, L- and D- $\gamma$ -glutamylmethylester and L- $\gamma$ -glutamyl-L-alanine are substrates for glutaminase B, which does not catalyze the hydrolysis and hydroxylaminolysis of asparagine.  $\alpha$ -Amino adipamic acid and  $\alpha$ -amino substituted amino acids are inert for both the isozymes. (4) The acylation step is rate-limiting in the catalytic reactions by both the isozymes.

**Excretion of Lysine by Lysine Sulfur Analog Resistant-mutants of *Candida pelliculosa*.** E. Takenouchi, D. K. Nikolova, K. Awano, K. Soda, and H. Tanaka. *Agr. Biol. Chem.*, **41**, 615 (1977).—The mutants of *Candida pelliculosa* resistant to S-( $\beta$ -aminoethyl)-L-cysteine (SAEC), a sulfur analog of L-lysine, excreted remarkable amounts of lysine in the medium. SAEC inhibits the growth of *C. pelliculosa* depending on the concentrations of SAEC, but L-lysine and L- $\alpha$ -aminoadipate restored the growth effectively. SAEC-resistant mutants (1726 strains) were induced from the wild-type strain of *C. pelliculosa* by UV irradiation or N-methyl-N'-nitro-N-nitrosoguanidine (NTG) treatment, and lysine productivity of the mutants was examined. Although the wild-type strain did not produce appreciable amounts of lysine extracellularly, almost all the resistant-mutants obtained did more or less. The several potent lysine producers excreted more than 2.2 mg/ml of lysine in the medium.

**Fermentative Production of CDP-Choline and Related Cytidine Coenzymes by Dried Cells of Yeasts.** A. Kimura, Y. Kariya, K. Aisaka, and T. Tochikura. *Amino Acid and Nucleic Acid*, **33**, 1 (1976), in Japanese.—CDP-choline and CDP-ester of aminoethanols were produced under the condition of yeast fermentation. The mechanism of the reaction was composed of two different systems. One was phosphorylation of CMP and aminoethanols by use of energy of yeast fermentation, and the other was condensation of CTP and phosphorylated aminoethanols.

Three important conditions were necessary for the fermentative production of cytidine coenzymes: 1) water content of yeast have to be lowered below than 30%, 2) presence of high levels of phosphate ions, 3) suitable concentration of glucose and CMP.

Intact cells of yeast could not phosphorylate CMP and could not form CDP-choline. Treatment of intact cells by triton X-100 was effective to phosphorylate CMP and to produce CDP-choline.

**Fermentative Production of CDP-Choline Analogues by *Hansenula jadinii*.** Y. Kariya, K. Aisaka, Y. Kaji, A. Kimura, and T. Tochikura. *Amino Acid and Nucleic Acid*, **33**, 4 (1976), in Japanese.—CDP-choline analogues were produced from CMP and choline analogues, *N*-substituted aminoethanols, with a dried cell preparation of *Hansenula jadinii* IFO 0987 by a fermentative process under a choline kinase-linked system. The yields of CDP-dimethylaminoethanol and CDP-diethylaminoethanol were comparable to that of CDP-choline; that of CDP-dimethylaminoethanol was somewhat higher. The yield of CDP-ethanolamine was as low as 20% of that of CDP-choline, even when phosphoryl ethanolamine was used instead of ethanolamine. The CDP-choline pyrophosphorylase in *H. jadinii* was active toward most phosphate esters of *N*-substituted aminoethanols, but not toward phosphorylethanolamine to form CDP-ethanolamine.

An elevated concentration of mono-, and dimethylaminoethanol inhibited glucose catabolism, aminoethanol phosphorylation and CDP-ester formation. Crystalline preparations of the sodium salt of both CDP-dimethylaminoethanol and CDP-diethylaminoethanol were prepared and characterized by chemical and physicochemical procedures.

***Meso*- $\alpha$ ,  $\epsilon$ -Diaminopimelate Dehydrogenase of *Bacillus sphaericus*.** H. Misono, H. Togawa, T. Yamamoto, and K. Soda. *Amino Acid and Nucleic Acid*, **34**, 63 (1976).—A new amino acid dehydrogenase catalyzing the oxidative deamination of *meso*- $\alpha$ ,  $\epsilon$ -diaminopimelate was found in the cell-free extract of *Bacillus sphaericus* IFO 3525. This dehydrogenase requiring NADP was specific for *meso*-diaminopimelate and the other isomers were not substrates. The enzyme was optimally active at about pH 10.5. NAD could not replace NADP.

**Properties of L-Methionine  $\gamma$ -Lyase from *Pseudomonas ovalis*.** H. Tanaka, N. Esaki, and K. Soda. *Biochemistry*, **16**, 100 (1977).—The distribution of bacterial L-methionine  $\gamma$ -lyase (L-methionine methanethiollyase (deaminating) (EC 4.4.1.11)) was investigated, and *Pseudomonas ovalis* (IFO 3738) was found to have the highest

activity of enzyme, which was inducibly formed by addition of L-methionine to the medium. L-Methionine  $\gamma$ -lyase, purified to homogeneity from *Ps. ovalis*, has a molecular weight of about 173,000 and consists of nonidentical subunits (mol wt: 40,000 and 48,000). The enzyme exhibits absorption maxima at 278 and 420 nm, and a shoulder around 330 nm, which are independent of the pH (6.0 to 10.0), and contains 4 mol of pyridoxal 5'-phosphate per mol of the enzyme. The formyl group of pyridoxal 5'-phosphate is bound in an aldimine linkage to the  $\epsilon$ -amino group of lysine residues of the protein. The holoenzyme is resolved to the apoenzyme by incubation with hydroxylamine, and reconstituted by addition of pyridoxal 5'-phosphate. The enzyme activity is significantly affected by both carbonyl and sulfhydryl reagents. L-Methionine  $\gamma$ -lyase catalyzes  $\alpha, \gamma$ - and  $\alpha, \beta$ -elimination reactions of, in addition to L-methionine, several derivatives of L-methionine and L-cysteine, e.g., L-ethionine, DL-methionine sulfone, L-homocysteine, and S-methyl-L-cysteine. The enzyme catalyzes also  $\gamma$ -replacement reactions of the thiomethyl group of methionine with various alkanethiols (C<sub>2</sub>-C<sub>7</sub>), arylthio alcohols (benzenethiol and  $\beta$ -naphthalenethiol) and the derivatives of ethanethiol (2-mercaptoethanol and cysteamine) to yield the corresponding S-substituted homocysteine. The thiomethyl group of S-methyl-L-cysteine also is replaced by ethanethiol to form S-ethyl-L-cysteine.

**Occurrence of meso- $\alpha, \epsilon$ -Diaminopimelate Dehydrogenase in *Bacillus sphaericus*.** H. Misono, H. Togawa, T. Yamamoto, and K. Soda. *Biochem. Biophys. Res. Commun.*, **72**, 89 (1976).—A new amino acid dehydrogenase catalyzing the oxidative deamination of meso- $\alpha, \epsilon$ -diaminopimelate was found in the crude extract of *Bacillus sphaericus* IFO 3525. This dehydrogenase requiring NADP was specific for meso-diaminopimelate and the other isomers were not substrates. The enzyme was optimally active at about pH 10.5. NAD could not replace NADP.

**Crystalline Inducible Kynureninase of *Neurospora crassa*.** K. Tanizawa, T. Yamamoto, and K. Soda. *FEBS Letters*, **70**, 235 (1976).—Kynureninase (L-kynurenine hydrolase, EC 3.7.1.3) catalyzes the hydrolysis of L-kynurenine to L-alanine and anthranilate, and plays an important role as a key enzyme of the aromatic and NAD pathways in tryptophan metabolism. The properties of partially purified kynureninase from a pseudomonad [1], *Neurospora crassa* [2] and rat liver [3] have been reported. Evidence for the occurrence of two types of kynureninase in *N. crassa* and their physiological functions were reported [4, 5]. Recently the enzyme has been purified to homogeneity from the extract of *Pseudomonas marginalis*, and crystallized [6, 7]. It was also demonstrated that kynureninase activity is under the control of  $\alpha$ -transamination of the bound pyridoxal 5'-phosphate (pyridoxal-P) catalyzed by the enzyme itself [8, 9].

In this communication, we describe the purification and crystallization of inducible kynureninase of *N. crassa* and some of its properties to compare with those of the bacterial enzyme.

**Purification and Crystallization of Bacterial  $\omega$ -Amino Acid-Pyruvate Aminotransferase.** K. Yonaha, S. Toyama, M. Yasuda, and K. Soda. *FEBS Letters*,

71, 21 (1976).—Although  $\omega$ -amino acids occur widely in a variety of animal tissues, plants and microorganisms in the free or conjugated forms [1], little attention has been given to the enzymic transamination of  $\omega$ -amino acids. Taurine- $\alpha$ -ketoglutarate aminotransferase was found in *Achromobacter superficialis* [2], purified to homogeneity, and crystallized to elucidate the physicochemical and enzymologic properties [3]. In addition to taurine, several other  $\omega$ -amino acids can serve as an amino donor, but  $\alpha$ -ketoglutarate is the exclusive amino acceptor in this amino-transferase reaction.

Recently we demonstrated the occurrence of a new  $\omega$ -amino acid aminotransferase, taurine-pyruvate aminotransferase, in the cell-free extract of *Pseudomonas sp.* F-126 [4].

In the present communication the purification, crystallization, and some properties of the enzyme are described.

**A New Oxygenase, 2-Nitropropane Dioxygenase of *Hansenula mrakii***  
—Enzymologic and Spectrophotometric Properties—. T. Kido and K. Soda. *J. Biol. Chem.*, **251**, 6994 (1976).—2-Nitropropane dioxygenase, purified to homogeneity from *Hansenula mrakii* (IFO 0895), has a molecular weight of approximately 62,000 and consists of two subunits nonidentical in molecular weight (39,000 and 25,000).

Stoichiometrical studies and the results obtained with  $^{18}\text{O}_2$  showed that 2 atoms of molecular oxygen are incorporated into 2 molecules of acetone formed from 2-nitropropane. In addition to 2-nitropropane, nitroethane, 3-nitro-2-pentanol, and 1-nitropropane are oxidatively denitrified.

The enzyme, which exhibits absorption maxima at 274, 370, 415, and 440 nm and a shoulder at 470 nm, contains 1 mol of FAD and 1 g atom of non-heme iron per mol of enzyme. The enzyme-bound FAD is reduced by 2-nitropropane under anaerobic conditions, but the enzyme-bound  $\text{Fe}^{3+}$  is not affected. The introduction of oxygen to the reduced form of enzyme causes reoxidation of the enzyme. The bound FAD and  $\text{Fe}^{3+}$  are reduced by the addition of nitromethane, which is not a substrate, under anaerobic conditions. The aerobic dialysis of the enzyme treated with nitromethane causes reoxidation of only the  $\text{Fe}^{2+}$ . Sodium dithionite also reduces both the enzyme-bound FAD and  $\text{Fe}^{3+}$  under anaerobic conditions. When the enzyme is dialyzed against 10 mM potassium phosphate buffer (pH 7.0) immediately after reduction by dithionite, the absorption spectrum similar to that of the native enzyme appeared with concomitant restoration of approximately 80% of the activity.

The enzyme activity is significantly inhibited by pyrocatechol-3,5-disulfonate disodium salt, 8-hydroxyquinoline, reducing agents such as 2-mercaptoethanol, and  $\text{HgCl}_2$ . The Michaelis constants are as follows: 2-nitropropane ( $2.13 \times 10^{-2}$  M), nitroethane ( $2.43 \times 10^{-2}$  M), 3-nitro-2-pentanol ( $6.8 \times 10^{-3}$  M), 1-nitropropane ( $2.56 \times 10^{-2}$  M), and oxygen ( $3.03 \times 10^{-4}$  M, with 2-nitropropane).

**Chromatography with Polymers.** K. Soda. *Kobunshi (High Polymer, Japan)*, **26**, 417 (1977), in Japanese.—Various aspects of chromatography with polymers and its application to biochemical studies are reviewed. Structures and properties of polymers used in gel chromatography, e.g., dextran gel, polyacrylamide gel and

agarose gel, are described to compare with each other. Affinity chromatography, which is widely used at present to purify enzymes, antigens, antibodies and hormones, also is explained with several examples. The principle and application of aqueous polymer two phase partition chromatography are described and discussed.

#### **A Novel Method for Sequencing Non-Radioactive Nucleic Acids.**

H. Sugisaki. *Bull. Inst. Chem. Res., Kyoto Univ.*, **54**, 156 (1976).—A simple and precise method for obtaining fingerprints from non-labeled nucleic acids has been developed. In this method, the 5'-hydroxyl groups of oligonucleotides produced by specific digestion of nucleic acids are phosphorylated with  $^{32}\text{P}$  in the polynucleotide kinase reaction and then fractionated by two-dimensional chromatography on polyethyleneimine (PEI)-cellulose thin layer plates. Under the condition used for fingerprinting, ( $\gamma^{32}\text{P}$ )ATP as phosphate donor stays near the origin, so that the reaction mixture for phosphorylation can be directly applied onto PEI-cellulose plates without removing ATP. This makes the fingerprinting procedure more simple and reproducible. It is also possible to deduce the sequences of non-labeled oligonucleotides precisely. This method will be very useful in studying the primary structure of nucleic acids.

#### **Sequences of Two Restriction Fragments Containing Promoters of Bacteriophage fd.**

H. Sugisaki. *Bull. Inst. Chem. Res., Kyoto Univ.*, **55**, 310 (1977).—In order to define the structure of DNA specifying the initiation of transcription (promoter), two restriction fragments each containing a strong promoter were isolated from bacteriophage fd replicative form DNA by the use of restriction endonucleases. One named *HapD-Hga1* was about 200 base pairs long and the other named *HapC-Hae1* was about 300 base pairs long.

The fragments were phosphorylated at the 5'-termini with polynucleotide kinase and ( $\gamma^{32}\text{P}$ )ATP. Following partial digestion either by an enzymatic method or by a chemical method, the sequences from the 5'-ends were determined, and the total sequences of the two restriction fragments were deduced in conjunction with the sequence information previously obtained from their transcripts.

By comparing the two promoter sequences where the RNA initiation sites in the sequences are aligned, a unique sequence TATAAT was found to locate around the tenth nucleotide upstream from the RNA initiation site. This TATAAT sequence is also contained in the corresponding region of other high level promoters, lac UV5 and SV40 DNA. It was concluded that the TATAAT sequence has an important role for the function of high level promoter.

#### **Studies on Bacteriophage fd DNA. IV. The Sequence of Messenger RNA for the Major Coat Protein Gene.**

K. Sugimoto, H. Sugisaki, T. Okamoto, and M. Takanami. *J. Molecular Biol.*, **111**, 487 (1977).—One of RNA species transcribed *in vitro* on phage fd replicative form DNA is initiated at a site preceding the major coat protein gene and terminated immediately after this gene. The total sequence of this RNA species was determined. The transcript was 369 bases long, and contained the sequence identical to the ribosome-binding site for phage f1 coat protein gene (Pieczenik, Model & Robertson, 1974) at positions 88 to 119 and the sequence for

coat protein at positions 175 to 324. The coat protein sequence was immediately followed by two termination codons UGA and UAA. The AUG codon appeared at the 5th and 23rd triplet-frame upstream from the codon for the first amino acid (Ala) of coat protein. The latter AUG codon was located in the middle of the ribosome-binding site. The result strongly suggests that coat protein is formed from a precursor containing 23 extra amino acid residues at the N-terminus. The transcript was mostly terminated with a sequence of eight U residues. It was also noted that a region of strong secondary structure is contained near the 3'-end.

**Cleavage Map of Colicin E1 Plasmid.** A. Oka and M. Takanami. *Nature*, **264**, 193 (1976).—Colicin E1 plasmid (ColE1) is a closed circular DNA molecule with a molecular weight of  $4.2 \times 10^6$ . ColE1 DNA has extensively been used as a molecular vehicle for cloning and amplification of DNA in genetic engineering. In order to expand such investigations, it is useful to make a cleavage map ordering ColE1 DNA pieces produced by bacterial restriction endonucleases. *Escherichia coli* RI restriction endonuclease (R. *EcoRI*) has been shown to cleave ColE1 DNA at a single unique site. We have now constructed a physical map with the *EcoRI* site as a reference point using two restriction endonucleases from *Haemophilus aegyptius* (R. *HaeII* and R. *HaeIII*).

**DNA Regions Essential for the Function of a Bacteriophage fd Promoter.** T. Okamoto, K. Sugimoto, H. Sugisaki, and M. Takanami. *Nucleic Acids Res.*, **4**, 2213 (1977).—The promoter for the major coat protein gene of bacteriophage fd contains a unique sequence, TATAAT, in the non-transcribed region corresponding to the Pribnow box. A R. *Hha I* cleavage site which destroys promoter function is located five base pairs upstream from the TATAAT sequence (fifteen base pairs upstream from the RNA initiation site). The promoter was cleaved into two fragments by R. *Hha I* and each promoter fragment was joined to DNA fragments derived from other regions. Ligation of the TATAAT-containing fragment to any of the DNA fragments examined resulted in recovery of promoter function. The results suggest for this type of promoter that no unique sequence is necessary upstream from the R. *Hha I* cleavage site although a contiguous DNA chain must be present in this area.

**Troponin Binding Region to Tropomyosin.** H. Ueno and T. Ooi. *J. Biochem.*, **81**, 1927 (1977).—Four fragments of  $\alpha$ -tropomyosin were prepared by specific cleavage at the Cys 190 by 2-nitro-5-thiocyanobenzoic acid and by tryptic digestion. These fragments were called the N-chain corresponding to residue 1 to 189 of the original chain, the C-chain from 190 to 284, the s-fragment from 13 to 149 and/or 128, and the p-fragment from 183 to 284, respectively. Fragments individually have little binding capacity to troponin as shown by gel electrophoresis. But a new band of the complex with troponin was detected using mixtures of the fragments, one from the N-terminal side and the other from the C-terminal side, *i.e.*, the N- and C-chains, the s- and p-fragments, the N-chain and the p-fragment, and the s-fragment and the C-chain. Therefore, the troponin binding region of tropomyosin is thought to be located between residues 150 and 190.